Received: 3 September 2021 | Revised: 19 May 2022 | Accepted: 28 May 2022

DOI: 10.1111/bre.12686

RESEARCH ARTICLE

Basin Research | IAS EAGE | WILEY

Sedimentation on structurally complex slopes: Neogene to recent deep-water sedimentation patterns across the central Hikurangi subduction margin, New Zealand

Adam Daniel McArthur[1] | **Adriana Crisóstomo-Figueroa**[1] | **Alex Wunderlich**[2] | **Alex Karvelas**[3] | **William D. McCaffrey**[1]

[1]School of Earth and Environment, University of Leeds, Leeds, UK

[2]OMV New Zealand Ltd, The Majestic Centre, Wellington, New Zealand

[3]WesternGeco, Schlumberger, Perth, Western Australia, Australia

Correspondence
Adam Daniel McArthur, School of Earth and Environment, University of Leeds, Leeds LS2 9JT, UK.
Email: a.mcarthur@leeds.ac.uk

Abstract

Deep-water sedimentation on active margins often entails complex sediment transport pathways through slope accommodation. Sedimentation in such settings is commonly differentiated into 'fill and spill' vs. 'tortuous corridor' models. To investigate the utility of these models in convergent settings 15,344 km^2 of 3D seismic data is used to investigate sedimentation and erosion patterns across the Hikurangi subduction margin. A series of thrust-bound trench-slope basins, each tens of kilometres long by kilometres wide, have been diachronously forming, filling and deforming through the Neogene until today. Five primary input points delivered sediment to the basins along the studied part of the margin. Channels display both axial and transverse orientations, the run-out lengths of which vary temporally. At various times, relatively coarse-grained sediment was trapped in the interior basins, occasionally then to be cannibalised during landsliding or erosion of growing structures. At other times, coarse-grained sediment was bypassed to distal basins or the trench. Multiple sediment input points and occasionally tortuous sediment dispersal corridors result in the evolution of convoluted depositional systems, often with similar styles of sedimentation occurring contemporaneously in proximal and distal basins, contrary to simple models of basin fill. A hierarchy of controls on sediment distribution can be distinguished. At the highest level, sediment distribution is controlled by external factors, for example, glacio-eustacy and tectonics. At basin scale, the interaction of sedimentary systems with local relief (e.g. evolving seafloor structures and landslides) dictates the location and style of deposition. At the lowest level, autocyclic factors (e.g. flow response to earlier deposits) influence the spatiotemporal variation in erosion and sedimentation. The complex interplay of these factors dictates whether basins were filling, spilling or some combination at any point in time, whilst basins that were filled and spilled may subsequently resume filling due to changes in the bounding conditions. Hence simple use of 'fill and spill' or 'tortuous corridor' models to tectonically active margins is not advised. Furthermore, as sedimentation may influence structure growth, constraining the controls on sediment distribution may improve understanding of the broader evolution of convergent margins and their resource distribution.

KEYWORDS

3D seismic, bypass, contourite, fault growth, mass-transport, trench-slope basin, turbidite

1 | INTRODUCTION

Understanding the evolution of flow pathways is critical for constraining sediment distribution, with implications for our knowledge of the transfer and storage of organic carbon (Rabouille et al., 2019), pollutants (Kane et al., 2020), and resources (Crutchley et al., 2019) in the deep sea. Sediment distribution pathways across tectonically active submarine slopes are complex (Bourget et al., 2011; Callec et al., 2010; Clark & Cartwright, 2009; McGilvery & Cook, 2004; Morley, 2009; Vinnels et al., 2010); in turn, sediment distribution may ultimately influence the structural evolution of active margins (Butler, 2019; McArthur, Bailleul, Mahieux, et al., 2021; McArthur & Tek, 2021; Noda, 2018).

Although it is clear that controls on deep-water slope sedimentation are complex and affected by numerous different factors (e.g. Prather, 2003), existing models that predict sediment distribution across structurally active slopes are necessarily simple (e.g. Sinclair & Tomasso, 2002; Smith, 2004; Sylvester et al., 2015). Generally, such models predict either bypass of proximal basins with subsequent back-fill (e.g. Beaubouef & Friedmann, 2000), relatively contemporaneous fill across multiple basins (e.g. Badalini et al., 2000; Bourget et al., 2011; Callec et al., 2010), or a systematic filling and spilling into downstream basins (e.g. Booth et al., 2003; Brunt et al., 2004; Deptuck et al., 2012; Marini et al., 2016; Pirmez et al., 2000; Prather et al., 2012; Prather et al., 2017; Satterfield & Behrens, 1990). The majority of these depositional models do not account for evolution of structure (excepting Ge et al., 2021), which may vary due to sediment delivery (e.g. McArthur, Bailleul, Mahieux, et al., 2021), hence variation in accommodation across the slope, as well as wider, external controls on the sedimentary and tectonic regimes. The conceptual models of fill and spill are best presented by Sinclair and Tomasso (Sinclair & Tomasso, 2002—their fig. 2), models of tortuous corridors by Smith (Smith, 2004—their fig. 5), contemporaneous deposition by Badalini et al. (Badalini et al., 2000—their fig. 5) and bypass with subsequent back-fill by Beaubouef and Friedmann (Beaubouef & Friedmann, 2000—their fig. 10). Many of the aforementioned studies are focused on the (near-) seafloor sedimentation patterns across active margin slopes (e.g. Bourget et al., 2011; Callec et al., 2010; McGilvery & Cook, 2004) or are focused on single sedimentary systems through geological time (e.g. Badalini et al., 2000; Beaubouef & Friedmann, 2000; Booth et al., 2003; McArthur, Bailleul, Mahieux, et al., 2021; Prather et al., 2012).

Highlights

- 3D seismic data used to map structures and sedimentary system evolution across subduction margin slope.
- Deep-water sedimentary response to structure growth is recorded by complex stratigraphic evolution.
- For example, turbidite channels, which run both axially and transverse to the slope, with highly variable run-outs.
- Sediment patterns don't conform to 'fill and spill' or 'tortuous corridor' models, relying on a range of controls.
- Variable structural character along margin partly inferred as result of sediment delivery/starvation.

Here, for the first time, we document the 3D stratigraphic evolution of sedimentary systems across an active convergent margin slope through geological time. This study documents the fill and deformation of nine slope basins, plus numerous minor depocentres, spanning 75 km along strike and 75 km down dip, from the Miocene inception of the basins to the present day. This is achieved by a detailed subsurface investigation of recently acquired, high-resolution 3D seismic data from across 15,344 km^2 of the central portion of the Hikurangi subduction margin, offshore eastern New Zealand (Figure 1), which allows us to reconcile concepts of continental slope sedimentation patterns across a convergent margin over geological

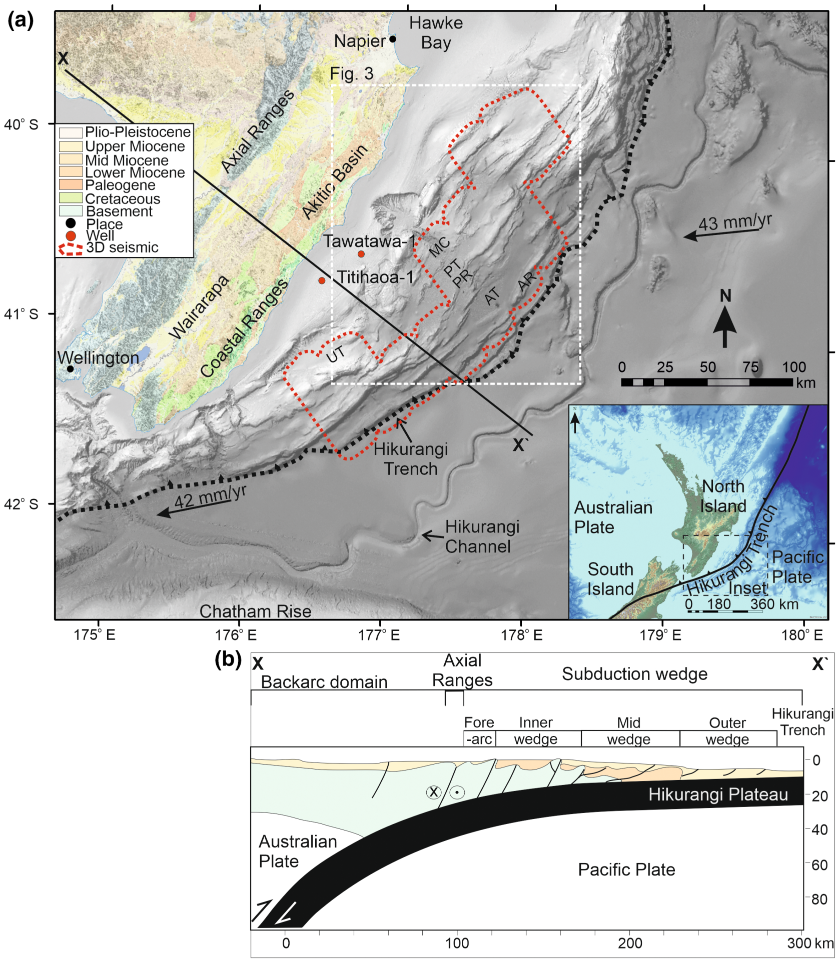

FIGURE 1 (a) Onshore geological map (Heron, 2014) and offshore 400 m grid resolution hillshaded bathymetry map (courtesy of NIWA) of the southern part of the Hikurangi Margin. This study is focused on area around the central part of the 3D seismic survey. MC—Madden Channel; PT—Pōrangahau Trough; PR—Pōrangahau Ridge; AT—Akitio Trough; AR—Akitio Ridge; UT—Uruti Trough. (b) Schematic cross-section of the Hikurangi subduction complex, modified from Nicol et al. (2007).

timescales. Structural interpretation married with identification of seismic facies and mapping of sedimentary sequences across the margin yield new insights into how deep-water sediment pathways interact with evolving growth structures, to both erode and deposit sediment across the intra slope basins and beyond. Here we define slope basins as true depocentres formed on the slope, rather than accreted trench fill (see McArthur et al., 2019 for distinction). The main aim of this work was to understand the tectonostratigraphic evolution of an actively evolving submarine slope on a convergent margin, with objectives:

- To complete structural interpretation and horizon mapping of 3D seismic data from the Hikurangi Margin of New Zealand.
- To identify and map sedimentary systems both temporally and spatially, and across and along multiple slope basins.
- To assess the controls dictating the sedimentary systems and any changes to them.
- Determine the validity of 'fill and spill' and 'tortuous corridor' models on active margin slopes.

2 | GEOLOGICAL SETTING

The modern Hikurangi subduction margin has developed over the last 25 Ma by convergence of the Pacific and Australian plates (Figure 1; Jiao et al., 2014; Nicol et al., 2007; Rait et al., 1991). The Hikurangi Margin is forming over an older accretionary prism (Mortimer, 2004; Spörli, 1980), subduction of which halted in the Cretaceous and was followed by a period of tectonic quiescence (Figure 2; Reyners, 2013; Strogen et al., 2014). The upper plate has experienced significant deformation through both subduction events, today presenting principally ENE-WSW-trending thrust faults, with subordinate normal and strike-slip faulting (Figure 3; Beanland et al., 1998; Chanier & Ferrière, 1991; Nicol et al., 2007; Wallace et al., 2009). Deformation has resulted in the development of a fold and thrust belt, with NE–SW elongated trench-slope basins developing on the back-limb of thrusts, which represent the depocentres on the slope (Figure 2; Bailleul et al., 2013; Barnes et al., 2010; Ghisetti et al., 2016; Lewis & Pettinga, 1993; McArthur et al., 2019). The resulting subduction complex is composite, with reactivation of older structures in the interior, thick-skinned

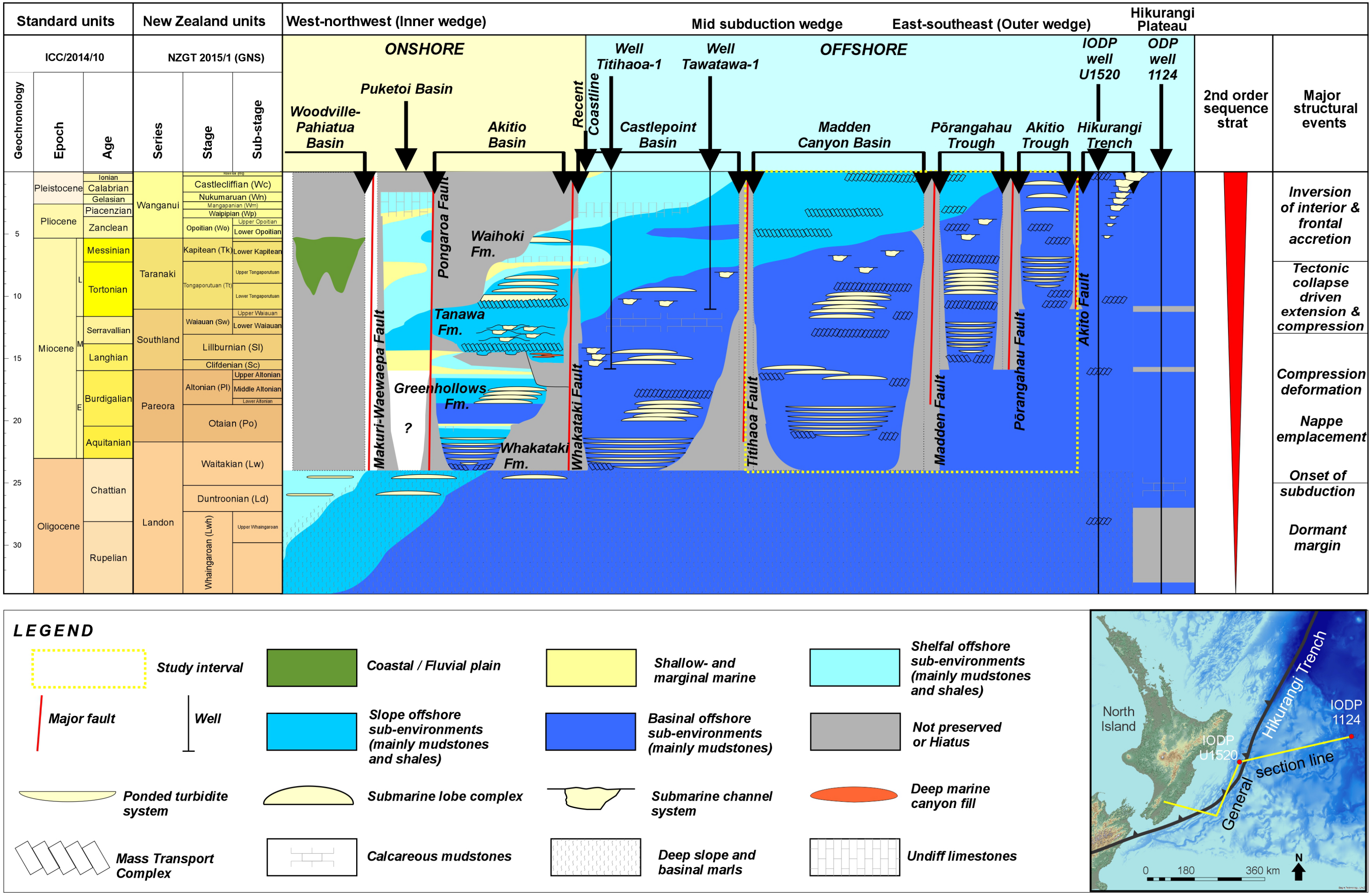

FIGURE 2 Tectono-stratigraphy of the Hikurangi Margin (modified from Bailleul et al., 2013; Barnes et al., 2020; Bland et al., 2015; Burgreen-Chan et al., 2016; McArthur, Bailleul, Chanier, et al., 2021; McArthur, Bailleul, Mahieux, et al., 2021; Tap Oil Limited, 2004; Uruski, 1997). Regional tectonism adapted from Rait et al. (1991), Lewis and Pettinga (1993), Chanier et al. (1999), Lee and Begg (2002), Nicol et al. (2007) and Reyners (2013). International time scale after Cohen et al. (2013), New Zealand stages after Raine et al. (2015).

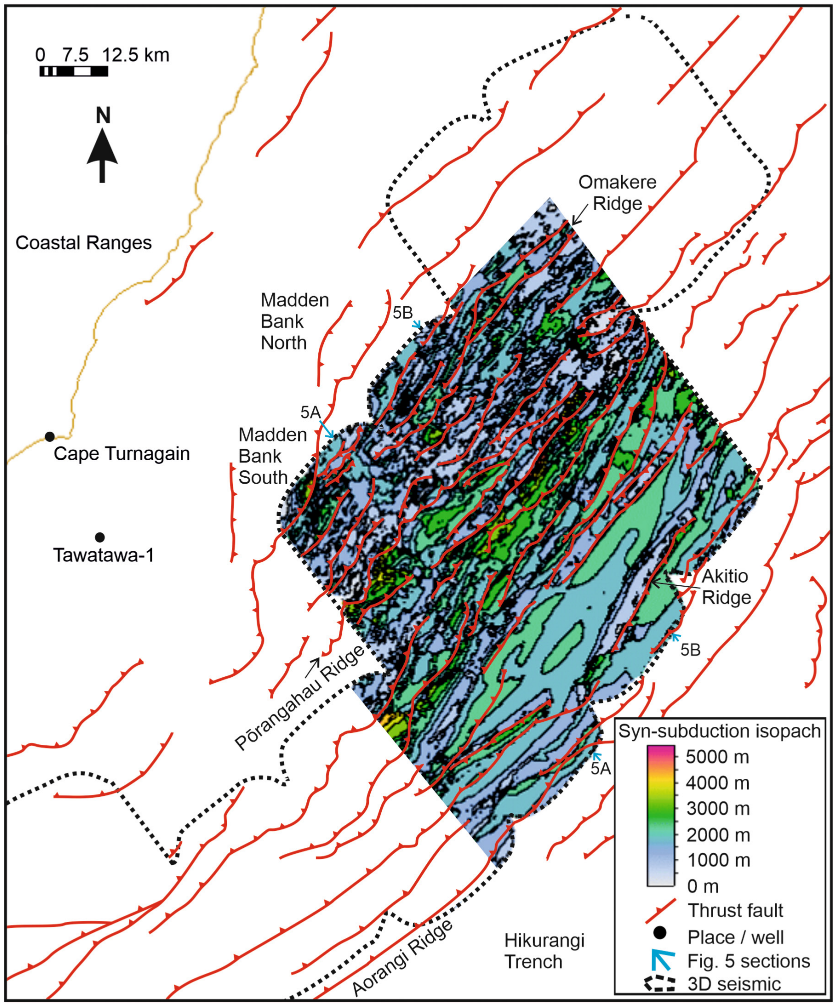

FIGURE 3 Isopach and structure map of the area of interest within the wider 3D survey. Structures adapted from Barnes et al. (2010); McArthur and McCaffrey (2019).

portion of the margin (McArthur et al., 2019), whilst deformation exhibits progressive migration through an outer area of thin-skinned deformation closer to the trench (Figure 4). However, out-of-sequence deformation is apparent (Figure 5; Bailleul et al., 2013; Ghisetti et al., 2016; Rait et al., 1991).

Three main stages of deformation are known in the Neogene, involving significant compression culminating in nappe emplacement during the Early Miocene (Chanier & Ferrière, 1991), mixed extension and compression in the Middle to Late Miocene (Barnes et al., 2002; Chanier et al., 1999) and renewed margin wide compression from the latest Miocene onwards (Nicol & Beavan, 2003). The Pliocene to recent evolution of the margin records significant shortening and uplift, resulting from acceleration of subduction (Nicol et al., 2007), which today is partly accommodated by strike-slip faulting and block rotations in the forearc (Beanland et al., 1998; Wallace et al., 2004), and frontal accretion (Barnes et al., 2010, 2018; Barnes & Mercier de Lepinay, 1997; Ghisetti et al., 2016; McArthur et al., 2019; McArthur & Tek, 2021; Plaza-Faverola et al., 2012).

The evolution of the subduction wedge is recorded by the fill of the trench-slope basins and development of their bounding structures; the innermost, exhumed, basins were filled with Miocene sediment, with generally younger strata deposited in more outward basins (Figure 2; Ghisetti et al., 2016; Lewis & Pettinga, 1993). Deep-marine sedimentation has predominated, particularly in the basins presently offshore (Burgreen-Chan et al., 2016; McArthur et al., 2019). The fill of the trench-slope basins includes deep-marine mudstones, siltstones and sandstones, deposited by (hemi-)pelagic and turbidity currents, mass-transport deposits, carbonates and contourites (Bailey et al., 2020, 2021; Bailleul et al., 2007, 2013; Crisóstomo-Figueroa et al., 2021; McArthur, Bailleul, Mahieux, et al., 2021; McArthur & McCaffrey, 2019; Paquet et al., 2011; Pettinga, 1982; Watson et al., 2020). True accretion is ongoing today at the deformation front, SE of the Akitio and Aorangi and ridges (Figures 3 and 5), with evolution of the deformation front at least partly dictating the location of the lower slope basins (Barnes et al., 2018).

The region investigated here and particularly its subsurface has received limited study. McArthur and McCaffrey (2019) documented a major channel system underlying the modern Madden Canyon and Channel. This

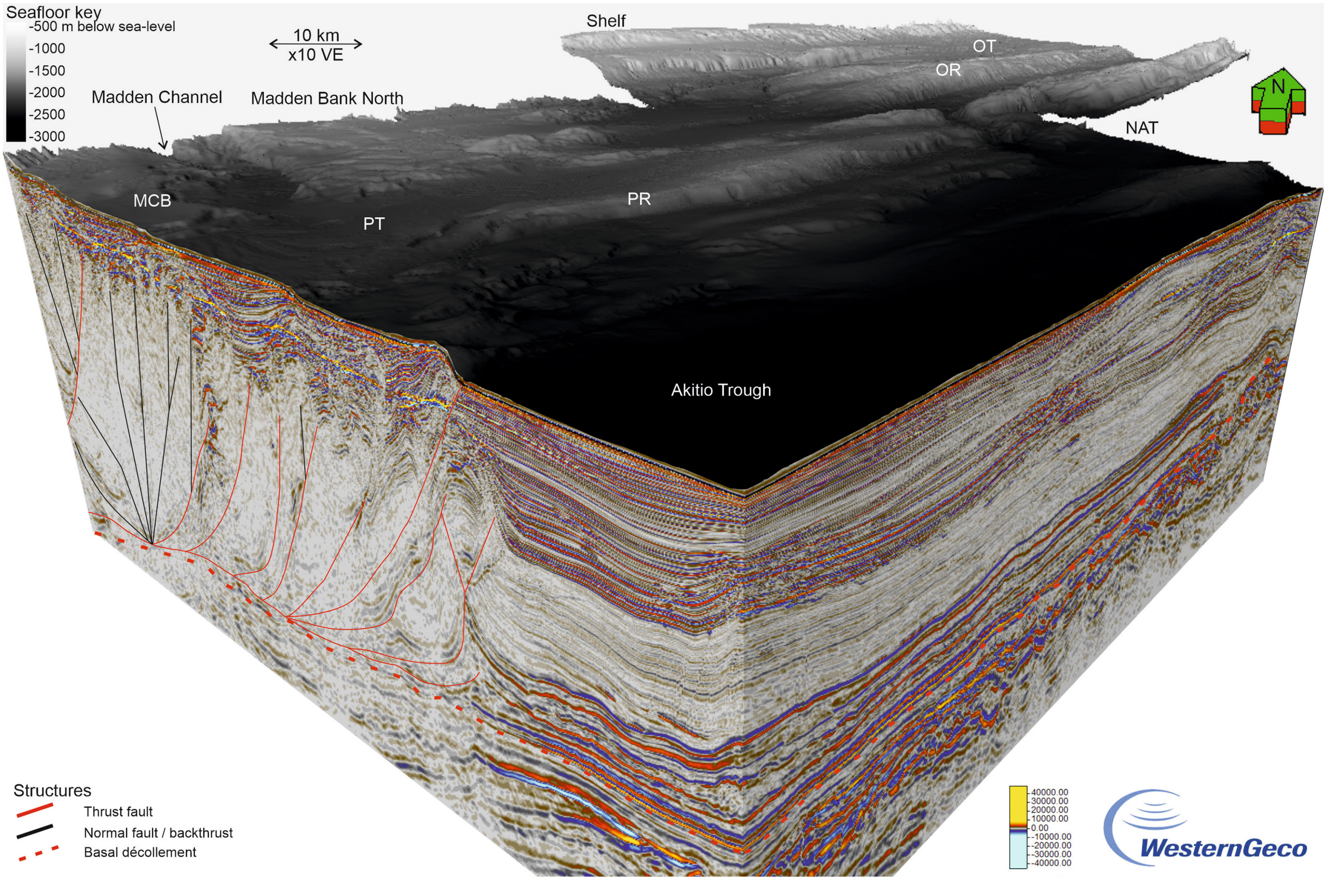

FIGURE 4 3D view of the study area seafloor (shaded depth m below sea-level) and with seismic cross-sections (displayed by amplitude). Note distinct change from thick-skinned style deformation in the interior, changing to thin-skinned deformation in the Akitio Trough. AT—Akitio Trough; AR—Akitio Ridge; MCB—Madden Canyon Basin; NAT—Northern Akitio Trough; OR—Omakere Ridge; OT Omakere Trough; PT—Pōrangahau Trough; PR—Pōrangahau Ridge; VE—vertical exaggeration.

conduit fed sediment into intra-slope accommodation during the Quaternary, including the Pōrangahau Trough (McArthur, Bailleul, Mahieux, et al., 2021). Limited observations on the stratigraphic architecture of the Akitio Trough are provided by McArthur et al. (2019), McArthur, Bailleul, Chanier, et al. (2021) and Bailey et al. (2020), and the Omakere Trough by Crisóstomo-Figueroa et al. (2021). These basins have a relatively simple internal structure (Barnes et al., 2010), with major basin bounding faults giving way to subtle folding and internal faulting, which is generally mild and convergent (McArthur et al., 2019).

3 | DATASET AND METHODS

15,344 km^2 of depth-converted 3D seismic data collected at broadband frequency by WesternGeco in 2017 was used to interpret the structure and stratigraphic architecture of offshore trench-slope basins (Figure 1). The dataset has an inline (NW-SE) and crossline (SW–NE) spacing of 25 m and a vertical resolution of 6.7 m at the mudline, reducing with depth to around 12 m resolution at 2500 m depth below the seafloor. For detailed interpretation the dataset was cropped to an area of interest covering the Madden Canyon, Omakere, Poanui, Pōrangahau and Akitio troughs (Figures 1 and 3), covering 6127 km^2. Major faults and structures were interpreted and regional surfaces were extrapolated from the full 3D survey using Petrel© E&P software; two well ties enabled the base Pliocene reflector to be picked by correlation through 2D surveys (Figures 1 and 5).

The cropped-volume was then interpreted using Paleoscan™ software. Paleoscan compares the seismic data trace-by-trace and establish links between horizon 'patches' with similar geophysical responses within a Model-Grid (Paumard et al., 2019). The similarities of adjacent wavelets are calculated and their relative distance in the Model-Grid permits the mapping of auto-tracked horizons. Over 500 horizons were generated from the base of the trench-slope basins to the seafloor, each manually quality checked and then geologically interpreted. Full stack data are displayed in SEG negative, such that a downward decrease in acoustic impedance is represented

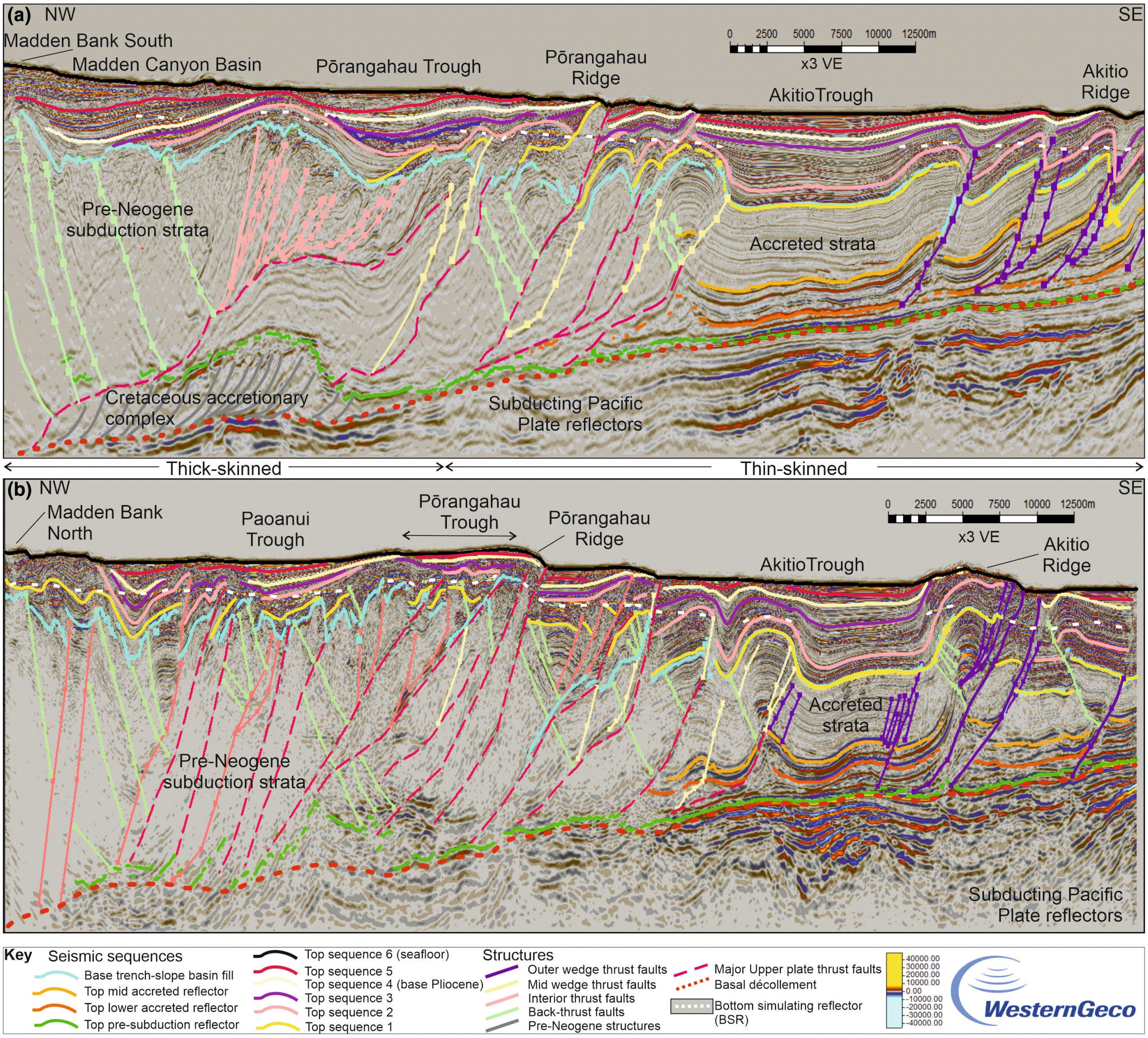

FIGURE 5 (a) Seismic dip-section illustrating the base of trench slope basin fill (blue horizon), above which detailed interpretations of seismic sequences were made (Figures 6–12) along an intersection of the Madden Channel. (b) Seismic dip-section 7.85 km to the NE showing the variable structure and basin fill along strike.

by a trough and a downward increase is represented by a peak.

Attribute mapping was used to create root-mean-square (RMS) of amplitude horizon maps for all of the 500 horizons (see Video 1), each with a calculation window of 7 ms, through the entire interval of interest and interpretations were manually checked with the horizons and with intersecting cross-sections to give confidence to the interpretation (see Supplementary Material S1 for uninterpreted regional cross-sections). RMS amplitude represents a measure of reflectivity and allows the detection of amplitude variations (Sheriff, 2002), which are interpreted to represent heterolithic intervals and as such significant changes in the strata, that is, mudstone to sandstone or vice versa. High amplitudes may also reflect hydrocarbon presence, with shallow gas (both free and hydrates) causing some interference in the uppermost sections of the outboard structures, for example the Akitio Ridge (Figure 4b; Supplementary Material S1B); such interference can be cross checked against other attributes and seismic cross sections (see Supplementary Material S2). Changes in RMS amplitude were examined by other attribute mapping and interpretations corroborated with cross-sections (see Supplementary Material S2). Overall, the 500 interpreted horizons can be separated into six seismic sequences (see Results). Selected horizons representative of each sequence (Figure 5) were then interpreted in terms of their structure and gross-depositional environments, as described below.

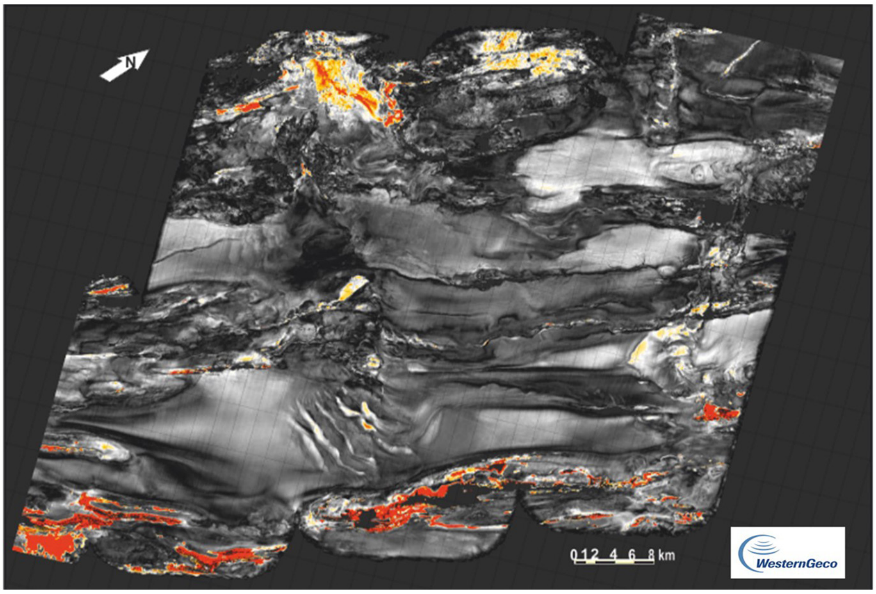

VIDEO 1 Video of RMS amplitude extractions moving from the interpreted basal synkinematic interval through five hundred intervals interpreted to the seafloor using Paleoscan. Data courtesy of WesternGeco. Green and white scale bar at bottom of video is 10 km long. To view this video please visit https://onlinelibrary.wiley.com/doi/10.1111/bre.12686.

4 | RESULTS

4.1 | Seismic facies

The seismic data permits distinction of different types of reflector infilling the trench-slope basins; packages of reflectors with comparable character allow definition of 14 seismic facies (Table 1; Figure 6). Seismic facies are defined by their amplitude, frequency, termination style and internal character. Their interpretation permits identification of depositional environments across the subduction slope. Those with relatively high amplitudes and bright RMS amplitude responses are interpreted as relatively coarse-grained, those being low amplitude with dull RMS amplitudes being fine-grained, which agrees with seafloor samples from the study area (McKeown, 2018). Groups of associated seismic facies may be interpreted in terms of a sedimentary system, for example, channels terminating in genetically associated lobes.

4.2 | Seismic sequences

The seismic facies, together with attribute mapping of seismic horizons are used to identify stratigraphic architecture and depositional environments; see Supplementary Material S2 for uninterpreted data. Therefore, significant changes in the reflector style across the margin allow the identification of time-equivalent seismic sequences, each bound by key reflectors, but not necessarily unconformities, which other than the basal syn-subduction unconformity, are not seen to be consistently present across the entire study area. A variety of seismic facies occur within each sequence. Below, the six seismic sequences are described then interpreted, each generally in terms of thickness and structure, then specifically in terms of the base, middle and upper part of the sequence. Attribute analysis was conducted to aid interpretation and outputs are displayed as RMS amplitude maps together with interpreted gross depositional environment maps (Figures 7–12; Video 1 and S2).

4.3 | Sequence 1—Lowermost preserved trench-slope basin fill (Figure 7)

4.3.1 | Observations

This sequence is absent to the NW, but is present to the SW, being up to 1 km thick in the Pōrangahau Trough (Figure 5), but patchy over structural highs (Figure 7a). Although present, sequence 1 is very thin (<50 m) to the east of the Pōrangahau Ridge (Figure 5). The extent of sequence 1 increases upwards through the sequence, to include reflectors in the north of the study area (Figure 7c,e). Structural activity is primarily recorded associated with the Paoanui and Pōrangahau ridges (Figure 7a), with the Omakere Ridge developing through the sequence (Figure 7c,e).

Above a sharp regional reflection, overlying chaotic, typically heavily deformed reflectors, the basal fill of the

TABLE 1 Seismic facies of the Hikurangi Margin subduction slope (Figure 6)

Seismic facies	Observation	Interpretations
Seismic facies 1—Pelagic to hemipelagic sediments	Low amplitude, low frequency, laterally continuous (where not truncated). Tens to thousands of metres thick, thousands to tens of thousands metres wide, with internally coherent reflectors. May be seen to onlap structural highs, fill palaeotopography and do not exhibit fluid anomalies	These are interpreted to represent background, mud dominated sediments (sensu Vinnels et al., 2010). May be separated into those draping ridges and those filling starved/perched basins
Seismic facies 2—Ponded strata	Alternating high and low amplitude, low to intermediate frequency packages seen to be thickening towards the centre of basins and onlapping at the margins	These are interpreted as alternating sand- and mudstone rich deposits filling basins and pinching out against basin margins, in the form of ponded turbidites (sensu Prather et al., 1998)
Seismic facies 3—Fine contourites	Mostly low amplitude, high frequency packages, semi-continuous but reflectors seen to both downlap basins and onlap structures, mostly contained within basins, but also seen to drape ridges. May display long wavelength, low amplitude sediment wave geometries	These geobodies with mounded geometries are interpreted as contourite drift deposits (sensu Faugeres et al., 1999). The low wavelength and low amplitude nature implies fine grain size (silt- or mudstone) (Wynn & Stow, 2002). Sediment was likely introduced by gravity currents and reworked by bottom currents (Bailey et al., 2020)
Seismic facies 4—Coarse contourites	Mixed amplitude, high frequency packages, semi-continuous within trench slope basins. May display short wavelength sediment wave geometries	These mounded packages are interpreted as contourite drift deposits (sensu Faugeres et al., 1999); when in close proximity to a channel they may form by overspill (Tek, McArthur, Poyatos-Moré, Colombera, Allen, et al., 2021). The short wavelength and often high amplitude nature implies coarse grain size (sand) (Wynn & Stow, 2002). Sediment was likely introduced by gravity currents and reworked by bottom currents (Bailey et al., 2020)
Seismic facies 5—Canyon fill	Mixed amplitude (often low to moderate amplitude intercalated with high amplitude, or chaotic), laterally discontinuous, high frequency reflectors. Tens to hundreds of metres thick, being up to 3500 m wide, but contained within larger bounding surfaces (up to 6 km wide) that incise reflectors of both basins and ridges	These deeply incising features, filled with a mixture of reflector types are interpreted as the fill of submarine canyons. These are interpreted to have been cut and filled in deep-water, as with those observed at outcrop and in bathymetric data on this margin (McArthur & McCaffrey, 2019)
Seismic facies 6—Starved channel fill	Mostly low amplitude, high frequency fill of incisions tens to hundreds of metres deep, by hundreds to thousands of metres wide, although typically less than 500 m wide. These typically run axially along basins. Features such as scours and bank collapse are apparent	These relatively small incising features with variable fill are interpreted as the fill of intra-slope submarine channel complexes that were starved of coarse-grained sediment (sensu Mayall et al., 2010). These are occasionally aggradational in form and may have laterally associated facies (SF8), or be more erosional with bypass of coarse-grained sediment

(Continues)

TABLE 1 (Continued)

Seismic facies	Observation	Interpretations
Seismic facies 7—Channel fill	Mostly high amplitude, high frequency fill of incisions tens to hundreds of metres deep, by hundreds to thousands of metres wide, although typically less than 500 m wide. These typically occur as transverse conduits, cross-cutting the structural ridges and occasionally being diverted axially. Features such as bar forms and bank collapse are apparent	These relatively small incising features with high amplitude fill are interpreted as the back-fill of intra-slope submarine channel complexes (sensu Mayall et al., 2010). These are occasionally aggradational in form and may have laterally associated facies (SF8) or contribute to supplying ponded or lobe sediments to basins (SF2 and 10)
Seismic facies 8—Overbank levees and terraces	Alternating high and low amplitude, high frequency bands of laterally thinning material hundreds thinning to tens of metres thick, often showing wave-forms with wavelength of hundreds to thousands of metres. Found laterally to seismic facies 6 and 7 and may display small scale deformation	This banded seismic facies, found adjacent to SF6 and 7 is interpreted as overbank levees (sensu Posamentier & Kolla, 2003) or terraces (sensu Hansen et al., 2017). Seen in association with intra-sub-basinal channels at outcrop, where often locally remobilised, occasionally observed in 3D
Seismic facies 9—Levee splay	Occurring adjacent to irregularities in SF8, these occur as laterally discontinuous, high amplitude, high frequency lobate deposits	These features are interpreted as splays due to erosion and break-out from levees, forming crevasse splay like deposits (sensu Posamentier & Kolla, 2003)
Seismic facies 10—Sand-rich lobe complexes	Imaged within intra-slope basins, mixed, mostly high amplitude but decreasing in a radial pattern, mounded features kilometres wide, by tens of metres thick, often stacking into packages hundreds of metres thick. Internally, reflectors may be seen to downlap towards the lateral margins	These mounded reflectors with coherent internal geometries are interpreted to represent submarine lobe complexes (sensu Prelat et al., 2009). They may represent either terminal lobes (McArthur, Bailleul, Mahieux, et al., 2021) or form part of a tortuous system of lobes migrating through slope basins (Burgreen & Graham, 2014)
Seismic facies 11—Fine-grained lobe complexes	Imaged within intra-slope basins, mostly moderate to low amplitude mounded, radial features kilometres wide, by tens of metres thick, often stacking into packages hundreds of metres thick. Internally, reflectors may be seen to downlap towards the lateral margins	These mounded reflectors with coherent internal geometries are interpreted to represent silty lobe complexes fed into the basins during intervals when coarse sediment was not available (sensu Boulesteix et al., 2019)
Seismic facies 12—Minor Mass Transport Deposits (MTDs)	Chaotic fill of irregular packages tens to hundreds of metres thick, often hundreds of metres to kilometres wide. Typically low amplitude and occur adjacent to structural ridges or within channels	These irregular, chaotic geobodies are interpreted to represent localised landslides resulting in mass-transport deposits (sensu Posamentier & Kolla, 2003), likely being shed from the growing ridges; as such they are probably mud rich
Seismic facies 13—Mass Transport Complexes (MTCs)	Chaotic fill of irregular packages tens to hundreds of metres thick, often kilometres to tens of kilometres wide, seen to interact with structural highs and channels, producing various kinematic indicators such as extensional features and compressional ridges. They may also display outsized clasts of coherent material, tens to hundreds of metres wide and thick and basal grooves and slide scars	These irregular, chaotic deposits are interpreted to represent major landslides, resulting in mass-transport complexes (sensu Posamentier & Kolla, 2003), that is, amalgamation of multiple MTDs. These may be seen to exploit channels or to spread across sub-basins. Shelf failures appear to be the main source of these large failures. However, margin scale collapses are also recorded (Collot et al., 2001)

TABLE 1 (Continued)

Seismic facies	Observation	Interpretations
Seismic facies 14—Strata built on top of MTCs	Seen overlying the irregular topography generated by MTCs (SF13) are packages of coherent reflectors, which thin towards and onlap the MTC relief. They are typically tens to hundreds of metres thick and kilometres wide, but show significant variations in thickness	These reflector packages are interpreted as sediment, likely turbidites, routed over and trapped on top of topography generated by MTCs (sensu Kneller et al., 2016)

trench-slope basins is typically low amplitude (SF1), interspersed with some distinct high amplitude features that define sedimentary systems (Figures 6a and 7a). A sedimentary system prograding from the north traverses the Paoanui Trough (SF7-8), terminating in the Pōrangahau Trough (SF10). Secondary systems are seen to enter the Madden Canyon Basin (SF10), both from the SW and north (Figure 7a).

Following this, in the middle of sequence 1, sedimentary systems enter the region from the NW/west (SF10-11), with the high amplitude system diminishing along the Paoanui Trough (SF2), and from the south following a trough axis (Figure 7c). The main depocentres were focused on the Madden Canyon Basin and Pōrangahau Trough (Figure 7c). The upper parts of sequence 1 exhibit dominant sediment input from the south-west (SF10-11), with minor input from the north and south (Figure 7e).

4.3.2 | Interpretations

The first sequence represents the earliest deposition in the newly forming trench-slope basins, which overlie a regional unconformity (Figure 5). As such, most basins were yet to receive substantial volumes of sediment, whilst erosion/non-deposition was occurring over the growing structures. The majority of all the imaged basins were starved of coarse-grained terrigenous sediment during their early formation, as indicated by their low amplitude, likely dominantly fine-grained deposits (Figure 7). Where not interpreted otherwise, these low amplitude, probably hemipelagic deposits, continued to blanket basins and ridges through all six sequences.

Although significant mass-wasting may be anticipated on the basin margins during their formation (e.g. Claussmann et al., 2021; McArthur, Bailleul, Chanier, et al., 2021), this is not observed here, potentially due to seismic resolution or lack of impedance contrast between the background sediments and potentially mud-rich debris flows (McArthur, Bailleul, Chanier, et al., 2021). The relatively long distance from the contemporary shelf, at least 10 km to account for Neogene to recent shortening (Nicol et al., 2007), would have limited potential for shelf-derived MTDs to reach the imaged basins at this time. Tentatively, based on well ties through 2D data, the basal fill is interpreted as Lower Miocene, which is comparable in age to the basal fill of the exhumed basins (McArthur, Bailleul, Chanier, et al., 2021) and the innermost offshore basins (Griffin et al., 2021). The outer basins, for example, the Akitio Trough were likely at least 10 km further offshore at this time (Nicol et al., 2007), with deformation and shortening focused on the Pōrangahau, Paoanui and Omakere ridges (Figure 7). Only the latter two of these structures are interpreted to have formed significant seafloor relief in the study area at this time, with the deformation front potentially sitting to the SE of the Pōrangahau Trough at this time.

Initially, the dominant sedimentary system was prograding from the north-northeast, along what is here termed the Paoanui System, representing an aggradational, somewhat tortuous system (sensu Smith, 2004), with a dominantly axial channel system (SF7) feeding perched lobes in the Paoanui Trough and terminal lobes (SF10-11) in the Pōrangahau Trough and the next depocentre downslope (Figure 7b; also see Supplementary Material S2i). Sediment routing was likely influenced by developing structural confinement, with the Pōrangahau Ridge already being apparent and likely having a seafloor expression (Figure 7b).

However, this sediment supply from the north was relatively short lived, with transverse routing from the west-northwest becoming dominant, including the proto-Madden System (McArthur & McCaffrey, 2019), depositing both coarse (SF10) and fine (SF11) grained lobes in the Madden Canyon Basin and Pōrangahau Trough (Figure 7d; also see Supplementary Material S2ii). Input and funnelling of sediment along the axis of troughs is seen from the SW and south, termed the Southern Axial System (Figure 7d), which is seen to merge with transverse systems in the Pōrangahau Trough (Figure 7d). Laterally offset compensational stacking of stratal elements (e.g. Doughty-Jones et al., 2019; Prelat et al., 2009), both of channels and lobes is not apparent, likely due to the relatively high levels of confinement within the narrow basins. However, migration of deposits, for

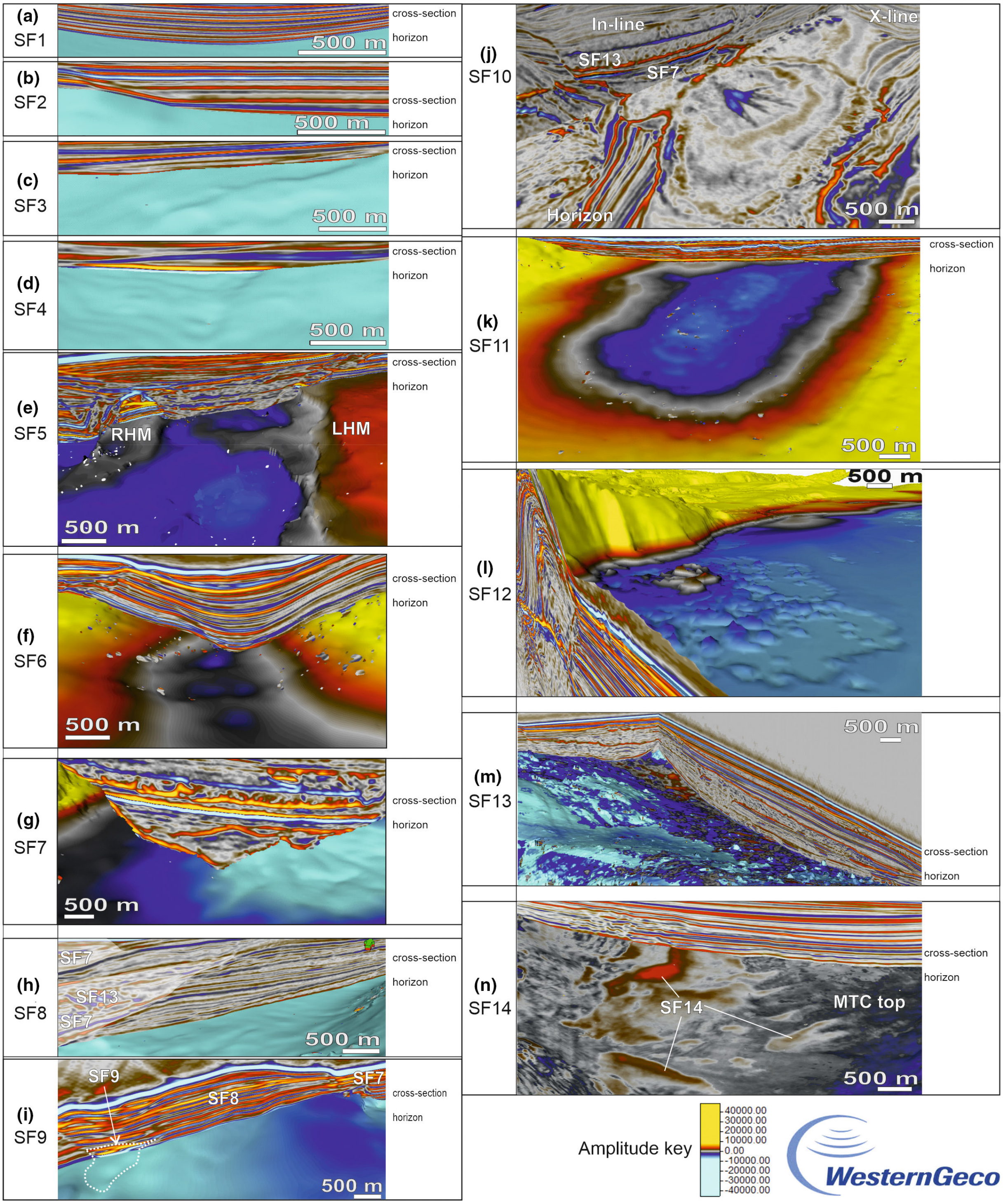

FIGURE 6 Illustrations of the seismic facies described in Table 1 in cross-section and horizon view. (a) Seismic facies 1—hemipelagic sediments. (b) Seismic facies 2—ponded strata. (c) Seismic facies 3—fine contourites. (d) Seismic facies 4—coarse contourites, which display higher amplitude basal surfaces, shorter wavelength and steeper crests than SF3. (e) Seismic facies 5—canyon fill, LHM—left hand margin; RHM—right hand margin. (f) Seismic facies 6—starved channel fill. (g) Seismic facies 7—channel fill. (h) Seismic facies 8—overbank deposits, which are the non-shaded parts. (i) Seismic facies 9—levee splay. (j) Seismic facies 10—sand-rich lobe complexes. (k) Seismic facies 11—fine-grained lobe complexes. (l) Seismic facies 12—minor Mass Transport Deposits (MTDs). (m) Seismic facies 13—major Mass Transport Complexes (MTCs). (n) Seismic facies 14—strata built on top of MTCs. All x3 vertical exaggeration. Further examples of the seismic facies and how they relate to the RMS amplitude extractions are in Supplementary Material S2.

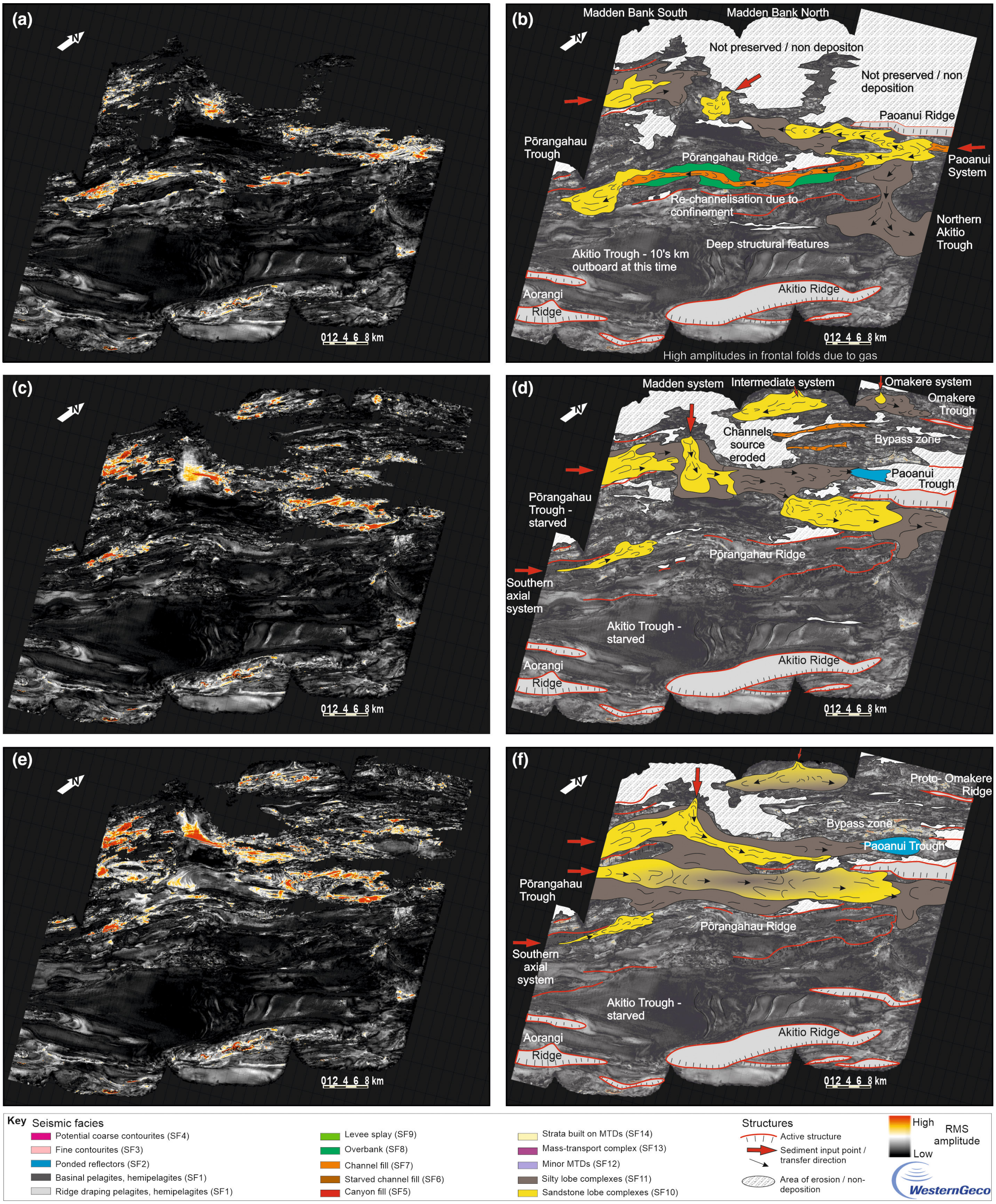

FIGURE 7 Mapped seismic horizons (RMS amplitude) and gross depositional environment interpretations of trench-slope basin fill sequence 1, showing (a) the basal fill of the trench-slope basins and its interpretation (b). (c) Stepping up through sequence 1 and its interpretation (d). (e) The upper part of sequence 1 and its interpretation (f).

example, lobes, along the basins is apparent (Figure 7), implying a tortuous style of sedimentation was present at times on isolated parts of this margin (Burgreen & Graham, 2014). A secondary sedimentary system, with input between the Madden and Omakere systems, here termed the Intermediate System, was feeding sediment into the northern Madden Canyon Basin (Figure 7d,f).

The Madden System became more prominent and amalgamated towards the top of sequence 1 (Figure 7f). Restriction of sediment supply to the Paoanui Trough led to ponding of sediments in this basin (SF2; also see Supplementary Material S2iii), as the rate of accommodation development linked to structure growth likely outstripped the capacity of the sediment flux to fill it (e.g. Marini et al., 2016). Sediment supply from the Southern Axial System was largely shut-off or diverted elsewhere at the top of this sequence.

4.4 | Sequence 2 (Figure 8)

4.4.1 | Observations

This sequence shows greater distribution than the first, but is thinner, being up to 750 m thick (Figure 5), although remaining patchy over structural highs (Figure 8a,c,e). Structural activity is recorded associated with all the major structures (Figure 8).

In the lower part of the sequence, the Madden System is dominant, feeding the proximal basins with sediments imaged as high amplitude responses (SF10-11), which are initially separated by areas of low amplitude responses (Figures 6b and 8a). Influxes of sediments imaged as high amplitude RMS responses (SF10) are also seen from the north, both along the Omakere Trough and between the Madden and Omakere Troughs, the latter of which also demonstrates chaotic (SF13) and ribbon-like (SF7) RMS responses (Figures 6m,g and 8a; also see Supplementary Material S2iv). These systems merge and contribute to the fill of the Paoanui Trough with SF2 and 10 (Figure 8a).

Subsequently, in the middle of sequence 2, sediments imaged as high amplitude responses flood the Madden Canyon Basin (SF10) and filter down into the Pōrangahau Trough (Figure 8c). Intercalations of chaotic and ribbon-like morphologies dominate in the Omakere, Paoanui and Northern Akitio troughs (Figure 8c; also see Supplementary Material S2v).

Finally, the upper part of sequence 2 shows chaotic RMS responses (SF13) representing sediments entering from the NW into both the Madden and Omakere depocentres, whilst the Pōrangahau and Northern Akitio troughs remain dominated by high amplitude SF10 with bright RMS responses (Figure 8e; also see Supplementary Material S2vi).

4.4.2 | Interpretations

Here the Madden System became established, feeding a series of tortuous, perched and terminal lobes (SF10) across the Madden Canyon Basin and Pōrangahau Trough, with ponding in the Paoanui Trough (Figure 8b). Flows were likely interacting with the developing structures, such as the Pōrangahau Ridge, with variable flow reflection, diversion and restriction apparent (e.g. Howlett et al., 2019; Soutter et al., 2021); one result of this topographic interaction is that the lobes in this interval appear to be disconnected from their feeder systems (Figure 8b; sensu Brooks et al., 2018). Fill of these basins was also supplied by activation of the Omakere System (SF7; Crisóstomo-Figueroa et al., 2021), which was interacting with MTCs (SF13) in the Omakere Trough (Figure 8b). These large scale MTCs may be the first shelf derived failures to be recorded in the study area. The Intermediate System was still active and appears to have propagated a channel into the Omakere Basin, fill of which was dominated by MTCs. A series of lenses and scours are interpreted to represent a channel-lobe transition zone (e.g. Hansen et al., 2021) in the west of the Paoanui Trough deposits (Figure 8b).

Moving up the sequence, the Madden System became trapped in proximal areas, potentially due to emplacement of MTCs in the area down dip of the lobes (Figure 8d). The Omakere System was fully established, with tortuous, transverse channels seen to avulse and interact with growth structures and MTCs, and systems with a distributary character within the axis of the troughs (Figure 8d). Although the Omakere System had only just initiated, it propagated into one of the most distal basins, in contrast to the other transverse systems that were mostly trapped in more proximal areas (Figure 8d).

Subsequently, at the top of sequence 2, the Madden System also became trapped in proximal areas, with some interaction of the sedimentary system with the MTC-top and deflection of the system northwards along the Pōrangahau Trough (Figure 8f). The Intermediate System was dormant or diverted elsewhere. Interaction of the Omakere System with MTC-top topography generated strata trapped and routed over the MTC tops (SF14). The Omakere System shows a rapid progradation through the trench-slope basins, producing lobes (SF10) in both the Poanui and Northern Akitio troughs (Figure 8d,f). Eventually, development of MTCs (SF13) along the Madden and Omakere systems led to a partial shutdown of these sedimentary systems, ending this cycle of sedimentation.

4.5 | Sequence 3 (Figure 9)

4.5.1 | Observations

Distribution of reflectors continues to improve compared to the previous sequence and sequence 3 is up to 800 m thick in the Akitio Trough (Figure 5), with deposition now covering most structural highs, except for the Omakere

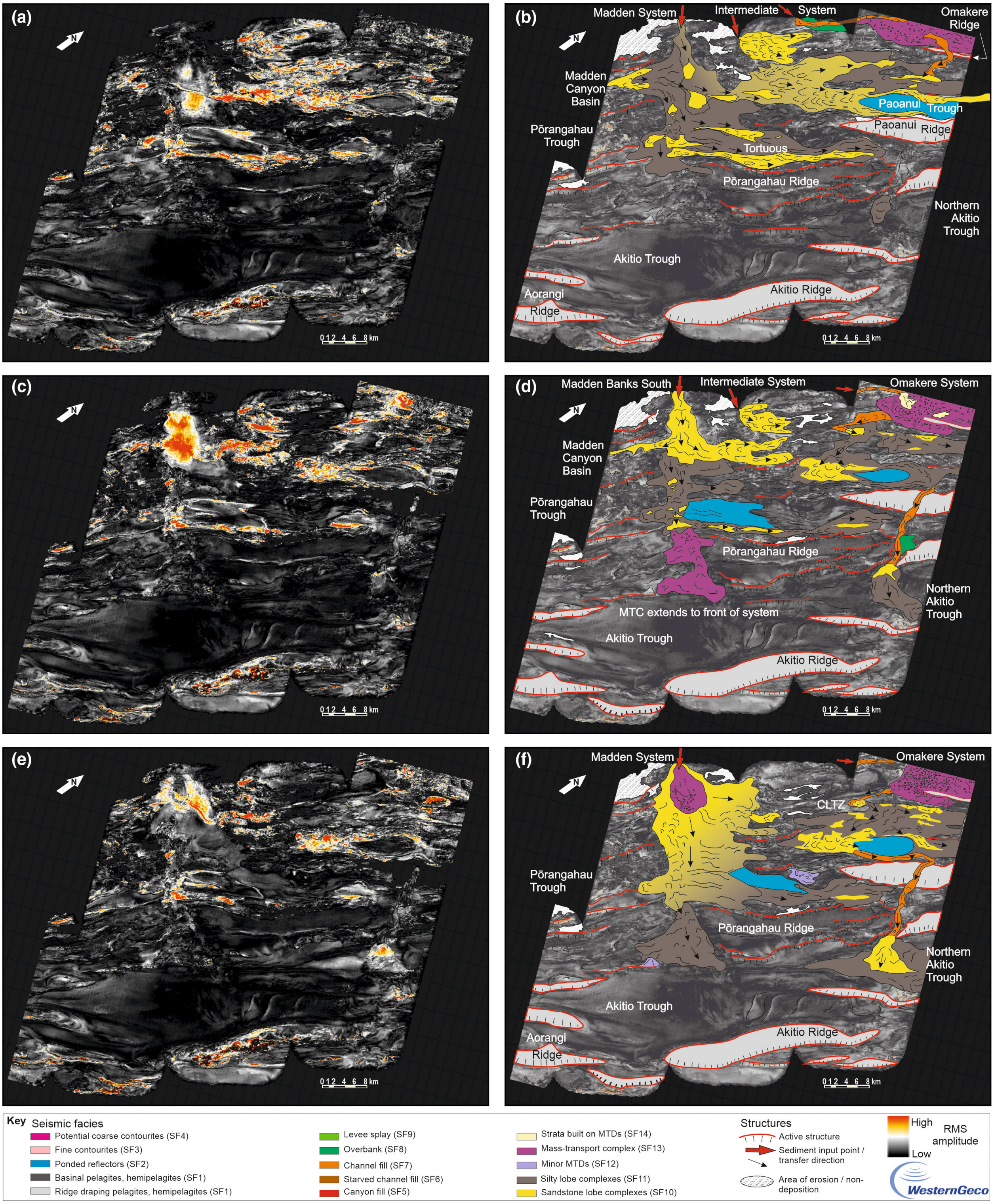

FIGURE 8 Seismic horizons (RMS amplitude) and gross depositional environment interpretations of trench-slope basin fill sequence 2. (a) the basal part of sequence 2 and its interpretation (b). (c) Stepping up through sequence 2 and its interpretation (d). (e) The upper part of sequence 2 and its interpretation (f). CLTZ, channel lobe transition zone.

and Paoanui ridges (Figure 9a,c,e). Reflectors are however seen to be truncated over the Akitio and Aorangi ridges (Figure 5). Activity is recorded associated with all the major structures (Figure 9); however, some areas, such as between the Pōrangahau and Akitio Trough exhibit less deformation than in previous sequences.

A significant reduction in high amplitude responses is seen at the base of Sequence 3, except SW of the Omakere

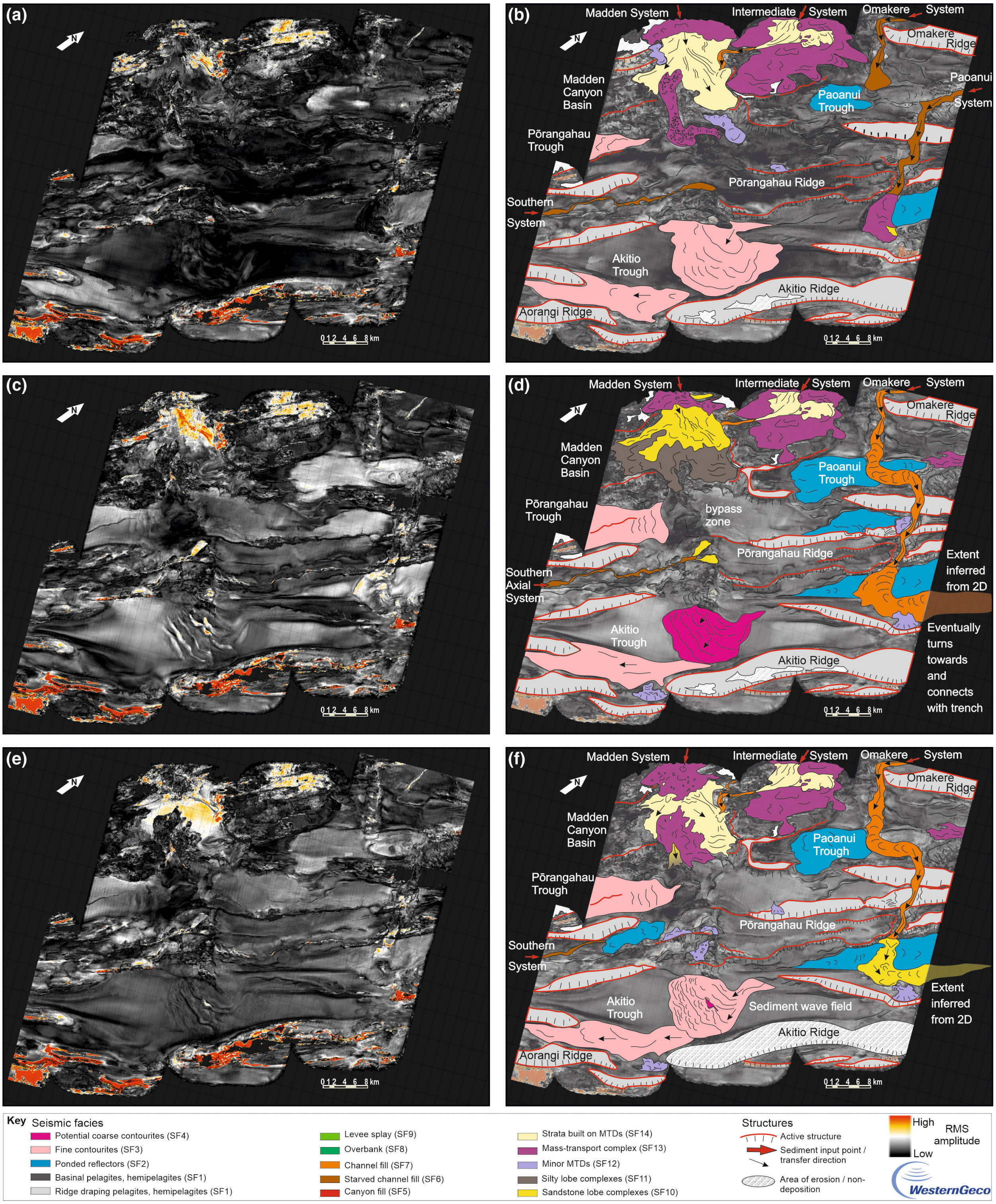

FIGURE 10 Seismic horizons (RMS amplitude) and gross depositional environment interpretations of trench-slope basin fill sequence 4. (a) the basal part of sequence 4 and its interpretation (b). (c) Stepping up through sequence 4 and its interpretation (d). (e) The upper part of sequence 4 and its interpretation (f).

Ridge, in the Paoanui Trough (SF14), and some isolated responses in the Madden Canyon Basin, including SF7, 8 and 9 (Figures 6g–i and 9a). Ridge-like RMS responses become prominent in the Akitio Trough (SF3; Figure 6c; also see Supplementary Material S2vii).

Subsequently, in the middle of sequence 3, erosion is apparent along the Madden System (SF5; Figure 6e; also see Supplementary Material S2viii), which terminates in stacked, high amplitude, RMS responses of SF10 in the Pōrangahau Trough and lower amplitude responses of

SF6 and 11 downstream (Figures 6j and 9c). More chaotic RMS responses (SF13) dominate the Omakere Trough, with muted RMS responses (SF2) in the Paoanui Trough and in a ribbon (SF6) extending from the Paoanui Trough to the Northern Akitio Trough (Figure 9c).

The upper part of sequence 3 shows continued development of high amplitude RMS responses at the end of the Madden System (SF10) in the Pōrangahau Trough, but with decreasing amplitude responses (SF11) at its downstream end (Figure 9e; also see Supplementary Material S2ix). The Omakere and Paoanui troughs, and smaller depocentres between those troughs and the Madden Canyon Basin become dominated by chaotic responses (SF13), whilst the Northern Akitio Trough shows dull responses (SF2) at the end of the ribbon-like feature (SF6) (Figures 6f and 9e).

4.5.2 | Interpretations

The Madden System almost shut-down between sequence 2 and 3, potentially due to reduction in sediment flux. Deposition of minor channel fills, with external levees and likely fine-grained lobes occurred, supplemented by sedimentation associated with resumption of the Intermediate System (Figure 9b). The emplacement of an MTC adjacent to the Omakere Ridge may have resulted in capture of subsequent turbidity currents of the Omakere System, potentially with ponding of turbidites on top of the MTC (e.g. Kneller et al., 2016). The radial, ridged reflectors in the Akitio Trough could be interpreted as contourites or sediment waves formed by gravity flows and that align sub-perpendicular to flow direction across the paleo-slope of a fan. The former interpretation is favoured as the waves appear disconnected from any turbidity current system, being as they initiate in the apparently sediment starved Northern Akitio Trough and migrate into the Akitio Trough (Figure 9b). Activation of contour currents on the margin was inferred to take place in the Late Miocene by Bailey et al. (2020), providing an indirect indication of the age of this sequence.

The Madden Canyon is seen to incise deeper and lower on the slope in the middle of sequence 3, which implies reinvigorated currents through the Madden System. This progradation of the Madden System coincided with the development of aggradational, structurally confined lobe complexes in the Pōrangahau Trough (Figure 9d; McArthur, Bailleul, Mahieux, et al., 2021). Flows along the Madden System at this time are interpreted to have been frontally blocked by seafloor bathymetry (e.g. Soutter et al., 2021), resulting in flow stripping and bypass of the fine parts of flows over the Pōrangahau Ridge (Figure 9d). This process of trapping sediment behind growth structures was invoked to drive sediment-structure feedback by McArthur, Bailleul, Mahieux, et al. (2021), whereby sediment loading focused stress on basin bounding faults, perpetuating their growth, which may account for the Pōrangahau Trough being one of the deepest basins on the margin (Figure 5). Mass-transport came to dominate the northern depocentres (Figure 9d), potentially as these areas in proximity to the shelf began to experience the effects of revitalised latest Miocene convergence (Nicol et al., 2007).

The Omakere Ridge had grown substantially by the top of sequence 3 and combined with emplacement of MTCs may have blocked or otherwise re-routed the Omakere System (Figure 9f). Sustained sediment delivery through the Madden Canyon resulted in very thick (ca. 300 m) aggradational lobe complexes in the Pōrangahau Trough (Figure 9f; McArthur, Bailleul, Mahieux, et al., 2021). Hence, the Madden System represented the main focus of sedimentation, before this sequence was shut-down by emplacement of MTCs, which were at first dominant in the north, but propagated southwards (Figure 9f).

4.6 | Sequence 4 (Figure 10)

4.6.1 | Observations

Reflectors are mostly preserved across the study area by sequence 4, which is up to 400 m thick, although thinning considerable onto the major structures, such as the Paoanui and Omakere ridges (Figure 5). Reflectors of sequence 4 are however truncated over the Akitio Ridge. Activity continues to be recorded associated with all the major structures, but with many structures in the centre of the study area becoming more prominent, for example the Pōrangahau Ridge (Figure 10).

Initially, the interior depocentres are dominated by chaotic RMS responses (SF13; also see Supplementary Material S2x), which are overlain by higher amplitude RMS responses (SF14) in places, and relatively low amplitude RMS responses (SF2) in the Paoanui Trough (Figure 10a). Low amplitude ribbons (SF6) are seen to extend across the Omakere and Paoanui troughs, and along the front of the Pōrangahau Ridge (Figure 10a). The sediment wave field in the Akitio Trough becomes enlarged and extends to the SE part of the trough, to run adjacent to the Aorangi Ridge (Figures 6a and 10a) as noted by Bailey et al. (2020, their Figure 10).

Successively, higher amplitude RMS responses (SF10) return to the Madden Canyon Basin, Pōrangahau Trough (Figure 10c). Concomitantly, a high amplitude ribbon (SF7) was extending across the slope from the Omakere to beyond the Northern Akitio Trough (see Supplementary

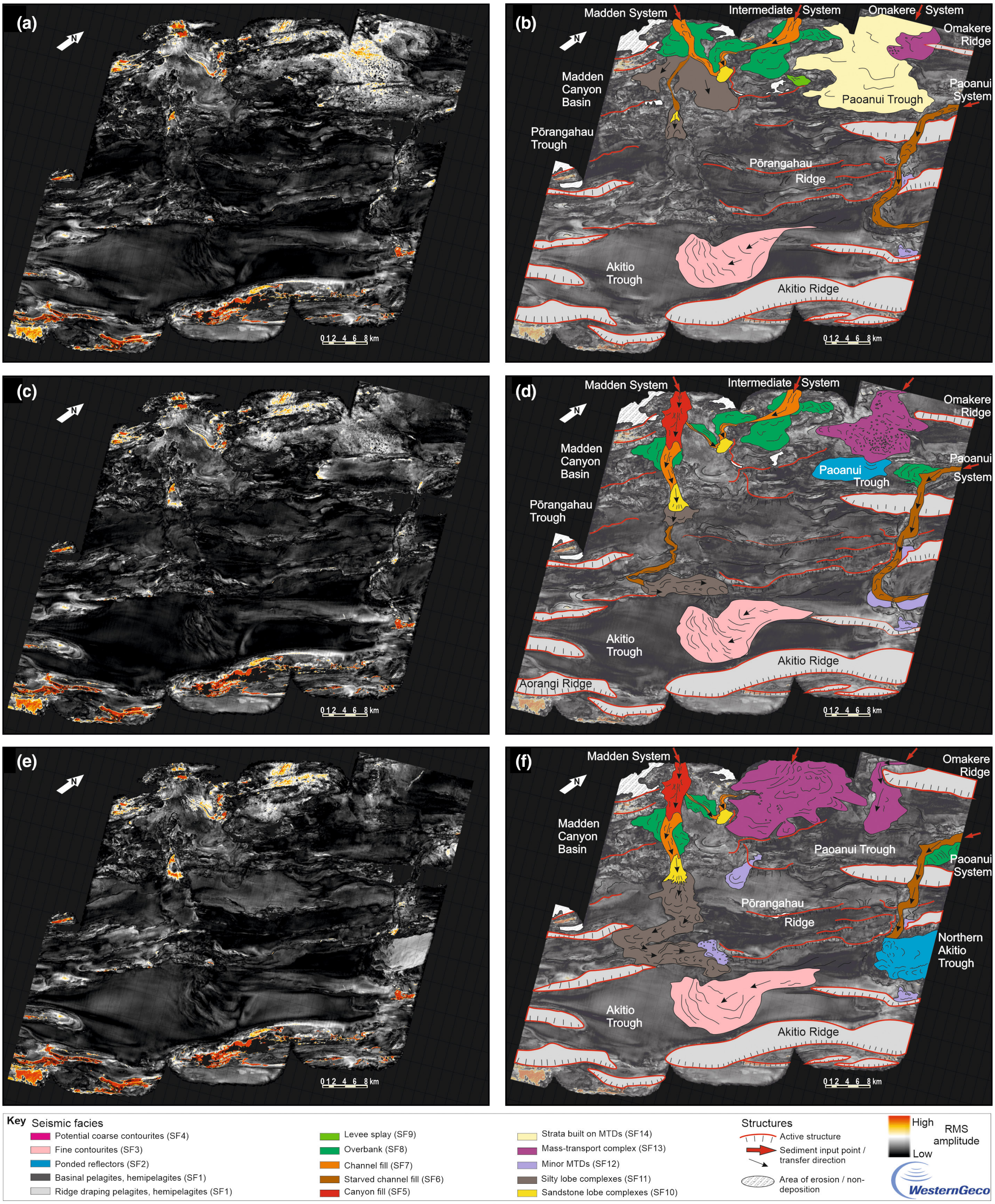

FIGURE 9 Seismic horizons (RMS amplitude) and gross depositional environment interpretations of trench-slope basin fill sequence 3. (a) the basal part of sequence 3 and its interpretation (b). (c) Stepping up through sequence 3 and its interpretation (d). (e) The upper part of sequence 3 and its interpretation (f). CLTZ, channel lobe transition zone.

Material S2xi), with development of intermediate amplitude RMS responses (SF2) in the Paoanui, northern end of the Pōrangahau, and Northern Akitio troughs (Figure 10c). Ridge-like RMS responses in the Akitio Trough briefly show higher amplitudes and shorter wavelengths (SF4) (Figures 6d and 10c); these occur at the end of a path of very low RMS responses with scalloped steps through the Pōrangahau Trough and Ridge into the Akitio

Trough (Figure 10c). Ridged reflectors are also present, but with low amplitude responses in the southern part of the Pōrangahau Trough.

In the upper part of sequence 4 appearances of chaotic reflectors (SF13) intermixed with high amplitude RMS responses (SF14) continue in the Madden and Intermediate systems (Figures 6n and 10e; also see Supplementary Material S2xii). High amplitude responses continue along the Omakere sediment pathway (SF7), but terminate in SF10 in the Northern Akitio Trough (Figure 10e). Moderate amplitude responses (SF2) are seen in the Paoanui Trough, whilst the ridges and troughs (SF3) observed in the Akitio Trough are dominantly low amplitude (Figure 10e).

4.6.2 | Interpretations

Sequence 4 began with resumption of sediment supply through the Madden and Intermediate systems, initially represented by sediments being routed over and likely trapped on top of the MTC topography generated at the top of sequence 3 (Figure 10b). The Omakere System apparently remained poorly supplied, feeding ponded sediments with moderate RMS responses in the Paoanui Trough (Figure 10b). The Paoanui System was again briefly active, albeit with limited sediment supply feeding mostly ponded deposits in the Northern Akitio Trough (Figure 10b).

The middle part of sequence 4, although still rich in MTCs, demonstrates resumption of sand supply, with an influx of sediment into the Madden Canyon Basin (Figure 10d). Structure growth in the mid-portion of the slope, for example, the Pōrangahau Ridge, may have helped trap sediment in proximal areas (Figure 10d). However, the Omakere System is seen to bypass the slope and connect with the trench in regional 2D seismic data (McArthur et al., 2019; see Supplementary Material S2xi). The Omakere System contributed to a ponded fill across its downstream basins (Figure 10d), whilst MTDs extending along the path of the Paoanui System may have blocked it. The Southern Axial System was again active and produced some small lobes in the accommodation between the Pōrangahau and Akitio troughs (Figure 10d). Low amplitude sediment waves in the Pōrangahau Trough may represent bottom current reworking of fine sediments in that relatively starved interval of the basin fill (Figure 10d). The high amplitude and shorter wavelengths of the Akitio Trough sediment wave field implies these contourites may be coarse-grained (Wynn & Stow, 2002), likely reworking material bypassed to the distal basin by turbidity currents; that is, representing a hybrid contourite—turbidite system (Bailey et al., 2020).

The top of sequence 4 is characterised by the emplacement of MTCs across all systems, with ponding of sediment with a high amplitude response on top of the Madden and Intermediate MTCs (Figure 10f). The Omakere System was active but had back-stepped to distribute sediment within the Northern Akitio Trough, where it terminated (Figure 10f); fine-grained sediments dominated in the Akitio Trough.

4.7 | Sequence 5 (Figure 11)

4.7.1 | Observations

Sequence 5 shows a condensation of reflectors towards and over many structures, being up to 500 m thick in the Madden Canyon Basin, but considerably thinner across most of the study area than previous sequences and is absent over the Akitio Ridge (Figure 5). The majority of the mapped structures continued to influence the thickness of the sequence, particularly with those to the north east, that is, top right of the maps becoming more prominent and closely spaced (Figure 11).

The base of sequence 5 sees a renewed occurrence of higher amplitude RMS responses (SF10), which develop progressively along the trend of the Madden System (Figure 11a). These high amplitude reflectors connect with a series of ridges that run axially along the Pōrangahau Trough (see Supplementary Material S2xiii). Chaotic RMS responses (SF13) continue to dominate in the Madden Canyon Basin and the Intermediate System, whilst high amplitude RMS responses of the Omakere System (SF7) terminate in lobate features (SF10-11) in the Northern Akitio Trough (Figure 11a). Low amplitude RMS responses, which display ridges and troughs (SF3) continue to develop in the Akitio Trough (Figure 11a).

In the middle part of sequence 5, chaotic reflectors (SF13) propagate down much of the Madden System, which connects to the Akitio Trough (Figure 11c; also see Supplementary Material S2xiv), terminating in high amplitude but areally-restricted RMS responses (SF10). The ridge and troughs continue along the Pōrangahau Trough (Figure 11c), but are now low amplitude (SF3). The Omakere System shows significant brightening of amplitudes, particularly in the slope traversing ribbon (SF7), perched in the Paoanui Trough (SF10), and terminal deposits (SF10-11) in the Northern Akitio Trough (Figures 6k and 11c).

The upper part of sequence 5 shows chaotic reflectors (SF13) along both the Madden and Intermediate systems, with some mixed amplitude RMS responses (SF7, 8 and 11) at the end of the Madden System (Figure 11e). Chaotic reflectors (SF12 and 13) become increasingly common in the Omakere System (Figure 6l), with high amplitude RMS responses restricted to the transverse ribbon (SF7) connecting

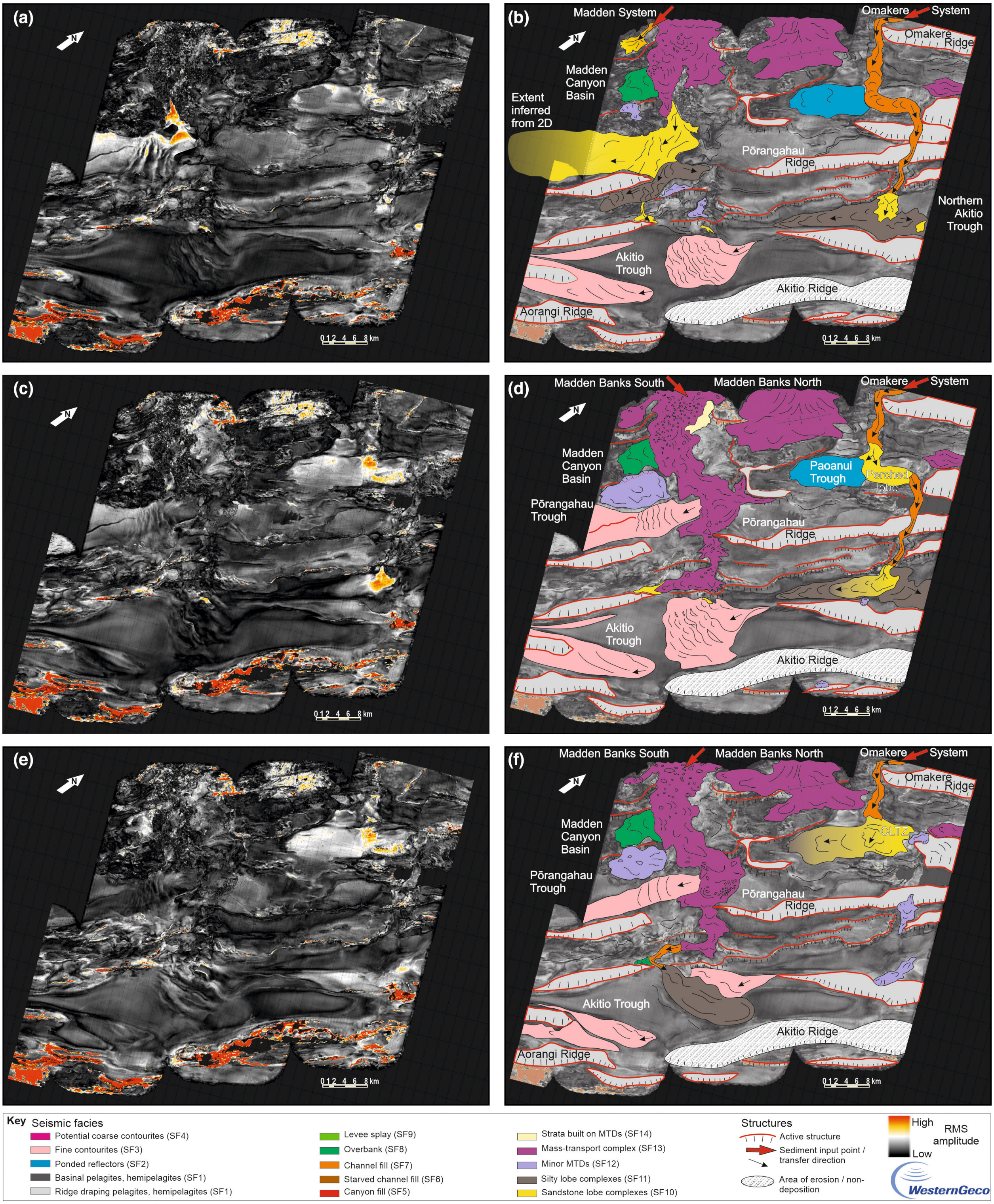

FIGURE 11 Seismic horizons (RMS amplitude) and gross depositional environment interpretations of trench-slope basin fill sequence 5. (a) the basal part of sequence 5 and its interpretation (b). (c) Stepping up through sequence 5 and its interpretation (d). (e) The upper part of sequence 5 and its interpretation (f). CLTZ, channel lobe transition zone.

the Omakere and Paoanui troughs, where high to moderate amplitude RMS responses (SF10-11) are seen in the Paoanui Trough (Figure 11e), but low amplitude responses in the Northern Akitio Trough (see Supplementary Material S2xv).

4.7.2 | Interpretations

The lower part of sequence 5 shows a resumption of siliciclastic sediment supply through the Madden System, with a less confined lobe system fed into the Pōrangahau Trough through the Madden Channel, the proximal part of which was dominated by MTCs (Figure 11b). The lobes in the Pōrangahau Trough display a distinct sediment wave morphology, which is perpendicular to the transport direction of the feeder conduit, indicating that bottom currents may have been reworking these deposits (Figure 11b; Bailey et al., 2020) or that flows were highly confined and funnelled along the trough, with enough energy to build seismically resolvable dunes. The Omakere System was depositing aggradational lobe complexes into the Northern Akitio Trough, but the Akitio Trough remained starved of gravity flow input and dominated by bottom current processes (Figure 11b).

The middle part of the sequence demonstrates significant amplitudes suggesting coarse-grained clastic transport along the Omakere System, supplying both perched lobes (sensu Plink-Björklund & Steel, 2002) in the Paoanui Trough and terminal deposits in the Northern Akitio Trough (Figure 11d). Mass-transport continued to dominate the upper reaches of the Madden System, but in general a propagation of this system fed its terminal deposits into the Akitio Trough (Figure 11d); this implies up-dip structures were either dormant or had been breached by gravity flows.

The upper part of sequence 5 shows major external and local MTDs dominating all depositional systems (Figure 11f). The Madden System may have been feeding channels and fine-grained lobes as far as the Akitio Trough, where they were likely being modified by bottom currents (Figure 11f). The Omakere System back-stepped to deposit lobes in the Paoanui Trough, which could have been a result of reduced sediment flux or blocking of the channel by landsliding (Figure 11f).

4.8 | Sequence 6 (Figure 12)

4.8.1 | Observations

Sequence 6 is largely contiguous across the study area, although absent across the major frontal structures, for example, the Akitio Ridge (Figure 5). This is overall the thinnest sequence but is up to 750 m thick in the Madden Canyon Basin (Figure 5). Structures that are visible on the seafloor influenced reflectors in this sequence, but many of the smaller structures seen at depth do not apparently affect this sequence (Figure 12).

The chaotic reflectors of sequence 5 are succeeded by moderate (SF8) to high amplitude RMS responses (SF5 and 7) along the Madden System, which terminate with RMS responses showing ridges and troughs (SF4) in the Akitio Trough (Figure 12a). Chaotic reflectors are seen in the former path of the upper reaches of the Omakere System, with a westwards shift in the high amplitude RMS responses (SF7), which propagate into the Paoanui Trough (SF10) and the Northern Akitio Trough (SF10 and 2).

The middle of sequence 6 exhibits high amplitude RMS response along the Madden System of SF5, 7 and 8, with significant accumulations of high amplitude RMS responses (SF10) in the Pōrangahau Trough and SF4 in the Akitio Trough (Figure 12c), both of which demonstrate ridges and troughs (SF3, 4 and 10; also see Supplementary Material S2xvii). Although dominated by chaotic reflectors (SF13), the Intermediate System shows some high amplitude ribbons (SF7) connecting to the Paoanui Trough (Figure 12c), where high amplitude RMS responses show ridge and trough structures (SF4).

The upper part of sequence 6 (Figure 12e), representing the last reflectors before the seafloor, only shows high amplitude but chaotic RMS responses in the proximal part of the Madden System (SF13), whilst the remainder of the system is relatively low amplitude (SF5, 8 and 11). Abundant high amplitude interference across the south-easterly part of the study area is due to shallow gas (Figure 4), which may occur as free gas or hydrates (Pecher et al., 2010). The Omakere System also exhibits dominantly low amplitude responses of SF6 and 11 (Figure 12e).

4.8.2 | Interpretations

At the base of sequence 6 re-incision of the Madden Canyon resulted in development of an asymmetrical channel-levee system, ultimately feeding a sediment wave field in the Akitio Trough (Figure 12b). The asymmetry of the levees and abundant sediment waves are interpreted to result from bottom current activity (Bailey et al., 2020), which in this case was interacting with the downslope gravity currents to modify the depositional architecture. Breakout and development of splays to the SW of the levee are apparent (see Supplementary Material S2xvi). A westward shift in the Omakere System is inferred to result from blocking of the conduit by MTCs, but the Omakere System remained well supplied, building lobes in the Paoanui Trough and the Northern Akitio Trough (Figure 12b). Growth of outer wedge structures may have helped to confined distal sediments, which show a ponded style in the Northern Akitio Trough (Figure 12b). The structures of the outer wedge demonstrate amplitude gaps, which represent areas of erosion of the growth structures.

By the middle of sequence 6, the Madden Canyon was firmly established, feeding sediment into the Pōrangahau Trough and downstream basins. Lobe-like reflectors

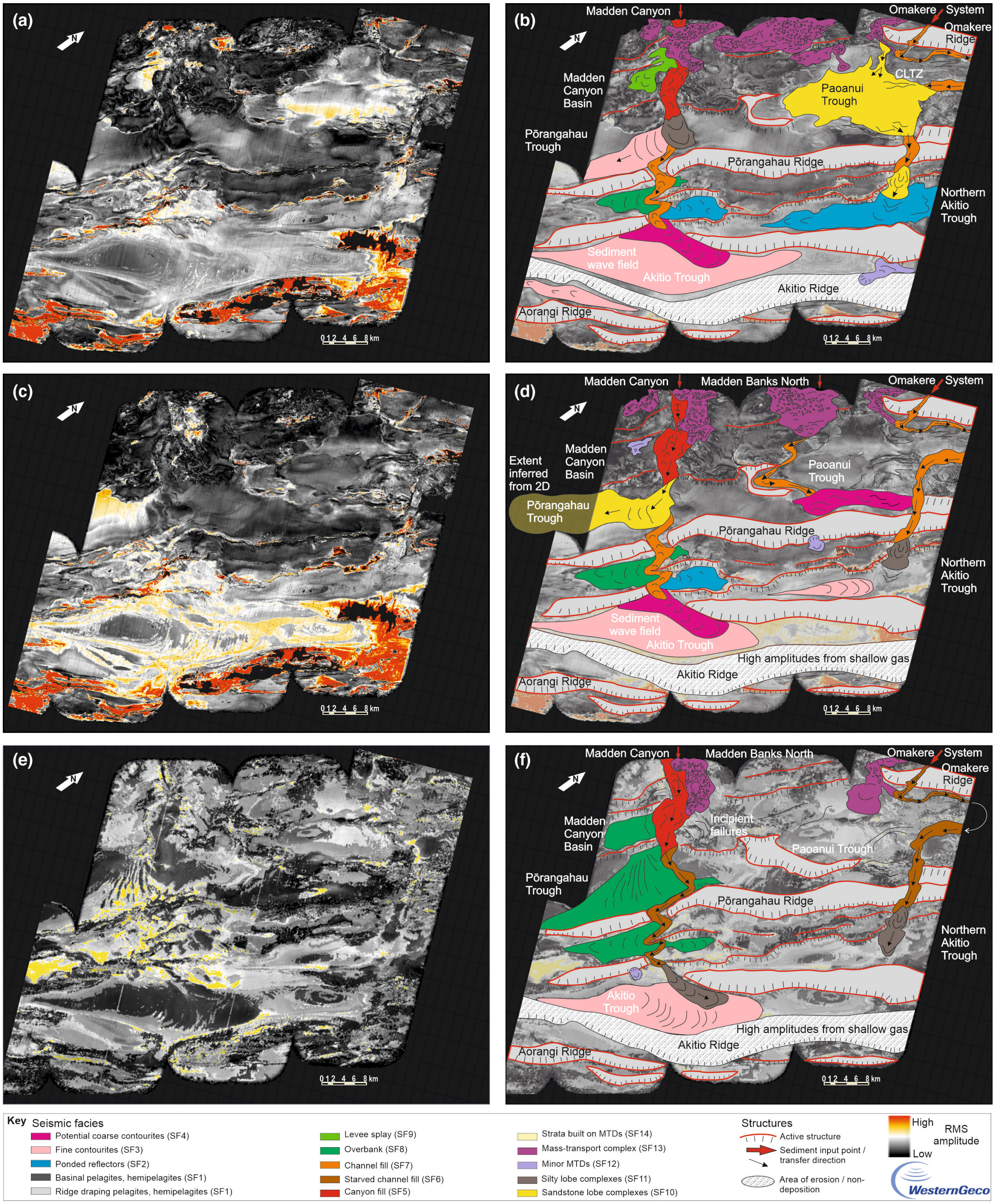

FIGURE 12 Seismic horizons (RMS amplitude) and gross depositional environment interpretations of trench-slope basin fill Sequence 6. CLTZ, channel lobe transition zone. (a) the basal part of sequence 6 and its interpretation (b). (c) Stepping up through sequence 6 and its interpretation (d). (e) The upper part of sequence 6 and its interpretation (f).

colonised by wave fields in the Pōrangahau Trough, asymmetry of Madden Channel levees, and the terminal deposits in the Akitio Trough, which display an elliptical pattern, all point to an influence of bottom currents modifying the gravity current dominated depositional system (Bailey et al., 2020). The Intermediate System shows a brief resumption, although dominated by MTDs, a channel is interpreted to propagate into the Paoanui Trough

(Figure 12d). The Omakere System was subsidiary at this time, supplying lobes interpreted as being mud-rich in the now structurally segmented Northern Akitio Trough (Figure 12d).

The uppermost part of the sequence represents recent sedimentation, which is dominated by fine, silty deposits (Crisóstomo-Figueroa et al., 2021; McKeown, 2018), with limited sediment supply during the present sea-level high-stand (Carter et al., 2002). The Madden Canyon was active, with knickpoint migration apparent across horizons (see Video 1), and connected to a downstream channel-levee system (see Supplementary Material S2xviii), although deposits associated with the modern Madden System are silty (McKeown, 2018) and only supplied fine-grained terminal lobes in the Akitio Trough (Figure 12f). Likewise, the Omakere System was relatively inactive, producing fine-grained lobes in the Northern Akitio Trough (Figure 12f). The present day starvation of the margin is not representative of its past, when large volumes of potentially coarse-grained sediment have been transported, both axially and transversally to be deposited all across the slope and occasionally beyond.

5 | DISCUSSION

5.1 | Sediment pathways through structurally complex deep-water bathymetry

This study of the evolution of sedimentary systems through complex and evolving seafloor bathymetry demonstrates at least five main entry points of sediment to the studied area of continental slope (Figures 7–12). Unlike sediment conduits described in other slope systems, for example, Brazos-Trinity system in the Gulf of Mexico (Prather et al., 2012), or systems described offshore Nigeria (Pirmez et al., 2000), or Angola (Doughty-Jones et al., 2019; Oluboyo et al., 2014), the entry points described here were not static, but show variation in activity and position; they also vary in the type of sediment they delivered.

The sedimentary systems supplied via these five input points also show significant variation in scale and style through the study interval. Unlike in the study of Howlett et al. (2021) a uniform evolution of channels was not seen, likely as structure growth was not uniform across the Hikurangi Margin. Canyon and channel systems are seen to variably extend across the slope, supplying sediment to otherwise isolated depocentres (e.g. the Northern Akitio Trough, Figure 12). Such sediment conduits may terminate abruptly (e.g. the Poanui Channel, Figure 7), or back-step to supply sediment higher up the slope (e.g. the Omakere System, Figure 11). Conversely, conduits may extend rapidly, bypassing the upper slope or even completely bypassing the entire slope to connect with the trench or basin plain (e.g. the Omakere System, Figure 10). At times, these conduits were significantly erosional, particularly when cutting growth structures, for example, the Madden Canyon (McArthur & McCaffrey, 2019). Shedding of volumetrically significant MTDs from growth structures also contributes substantially to the fill of slope-basins (Figure 8), hence at times the source of basin fill sediment may be considered to be 'in the sink', by cannibalisation of sediments deposited on previously undeformed areas of the margin.

Fundamentally, the concepts of basins either filling and spilling (e.g. Sinclair & Tomasso, 2002), or bypass of proximal intra-slope basins with subsequent back-fill (e.g. Beaubouef & Friedmann, 2000), or sedimentation through tortuous corridors (e.g. Smith, 2004), are over-simplistic end members. An overview of a wide area of the continental slope is required to make assessments of regional sediment distribution; such large 3D seismic datasets have only recently become available (e.g. this study; Naranjo-Vesga et al., 2020; Paumard et al., 2020). At any one time sedimentary systems may be filling parts or all of an intra-slope basin, whilst other sediment conduits may be bypassing that basin to feed downstream basins, both on the slope or beyond (Figure 13). Abrupt shutdown of a sediment conduit may then result in starvation of previously well supplied depocentres, whilst switching or migration of conduits may lead to sediment supply in other, previously starved areas of the slope. These patterns of sedimentation and bypass are further complicated by structure growth, emplacement of MTDs and autogenic changes to the sedimentary system restricting or diverting sediment elsewhere on the slope (Figure 13). Moreover, slope basins that were 'filled' may see renewed creation of accommodation, once more trapping incoming sediment. Hence, at any time, any basin may be filling, spilling and/or bypassing, and may switch between these states due a variety of controls. Furthermore, although tortuous corridors are seen in this dataset, these were transient features, persisting until some of the above-mentioned modifications of the sedimentary system disrupted the corridor.

5.2 | Controls on sediment distribution on tectonically active margins

A range of mechanisms has been invoked to influence the sediment distribution across active margins (e.g. Bourget et al., 2010; Naranjo-Vesga et al., 2020; Stow et al., 1985; Tek et al., 2020; Tek, Mcarthur, Poyatos-Moré, Colombera, Patacci, et al., 2021; Watson et al., 2020). Based on our

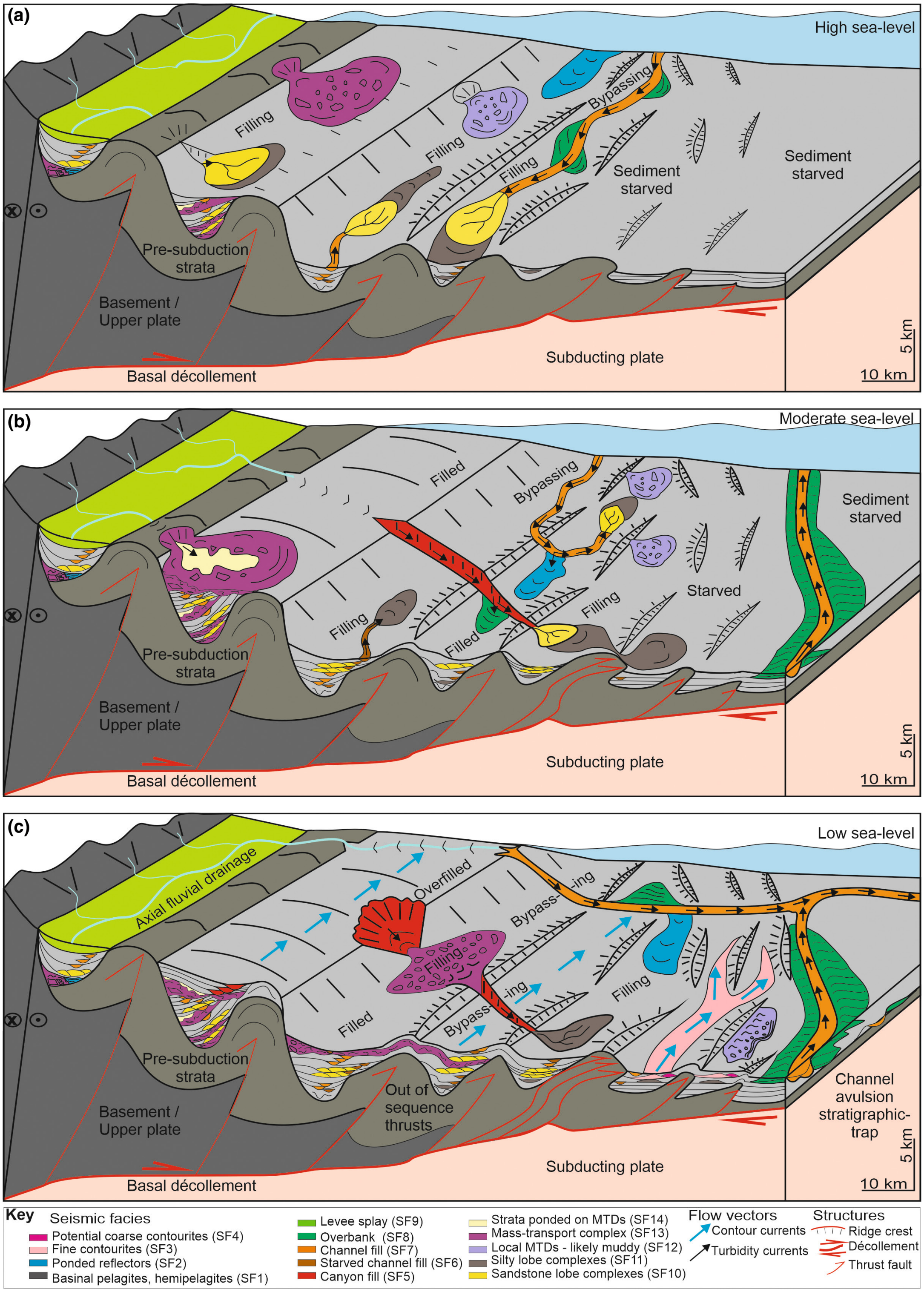

FIGURE 13 Schematic illustration of sediment pathway variation through tectonically active submarine slopes. (a) Relatively simple sedimentation patterns may exist early in the development of an active margin, with both axial and transverse sediment distribution. (b) Developing structures and associated landsliding creates topography with which deep-water sediment conduits may interact. (c) At any one time a basin may be filled, filling or being bypassed by a sediment conduit and may switch between these states due to a variety of external, local and autogenic controls (shown on the figure and discussed in the text). Sea-level variations are for illustrative purposes only.

observations here, these are assigned to a distinct hierarchy of controls. At the highest level, the overall form of the Hikurangi Margin and its accommodation is provided by tectonic forcing (McArthur et al., 2019), which also largely dictates slope gradients. Other external forces at the margin scale include regional sediment flux, climate, eustatic sea-level and contour current activity; in combination these determine the overall sediment supply and influence its distribution across the region, and hence whether or not basins are supplied with coarse terrigenous sediment (Figure 13). At basin scale, local forcing, such as growth of bounding structures, emplacement of mass-transport complexes, breach of structures by sediment conduits, and fill of local accommodation, all contribute to determining whether an area of a basin is filling, spilling or starved of sediment due to bypass to downstream depocentres (Figure 13). A third level of autogenic regulation of the sedimentary system exists, for example, through the effects of flow stripping at sills (see sequence 3; Sinclair & Tomasso, 2002), levee breaching (see sequence 6; Posamentier & Kolla, 2003), knickpoint migration in channels (Tek, Mcarthur, Poyatos-Moré, Colombera, Patacci, et al., 2021) and canyons (see Madden Canyon in sequence 6), channel avulsion (see sequence 2; Armitage et al., 2012), and of variable flow characteristics such as flow depth, density and transported grain size (Crisóstomo-Figueroa et al., 2021), the latter of which are below the resolution of seismic studies.

Feedback loops between sediment supply and structure growth may influence the tectonic development of individual basins, perpetuating generation of accommodation (McArthur, Bailleul, Mahieux, et al., 2021), leading to prolonged fill of the interior basins (McArthur, Bailleul, Chanier, et al., 2021). This is apparent in the Pōrangahau Trough and North Akitio Trough in the present study (Figure 8d,f). Although intricately linked to it, the effects of MTD emplacement can override tectonic forcing, for example, the MTD that blocked the Omakere System and forced its channel to cut closer to the crest of the Omakere Ridge (Figure 12). These factors may lead to similar facies belts occurring almost with random temporal and spatial distribution across the margin.

The controls on the distribution of sediment on active margins inherently dictate the distribution of petroleum systems elements, both for conventional hydrocarbons and emerging resources, such as gas hydrates. For example, fluid migration pathways are largely governed by structures on the Hikurangi Margin (Barnes et al., 2010), whilst conventional reservoirs are concentrated in specific areas due to interaction of sedimentation and structure growth (McArthur, Bailleul, Mahieux, et al., 2021). Whilst gas hydrate distribution on the margin is tied with growth folding (Crutchley et al., 2019), potentially economic accumulations require suitable host lithologies and seals (e.g. Hillman et al., 2017).

5.3 | Implications for sediment structure interaction and basin evolution

Large scale 3D seismic surveys along extensive portions of active margins are beginning to permit new insights into sediment—structure interactions (e.g. Chen et al., 2021; Ge et al., 2020; McArthur, Bailleul, Mahieux, et al., 2021; Naranjo-Vesga et al., 2020). Under the correct conditions of sediment supply and active tectonics, interactions of growth structures and sedimentation may arise (Storti & McClay, 1995). Here, as with other active margins (e.g. de Sagazan & Olive, 2021; Masek & Duncan, 1998; McArthur, Bailleul, Mahieux, et al., 2021; Olive et al., 2014; Willett, 1999; Worthington et al., 2018) influxes of sediment into a basin are seen to subdue and even terminate active faulting within a basin, focussing stress onto basin bounding faults (Figure 14). However, this process is not uniform along the length of a basin, with sediment structure interactions being focused on the parts of the basin where sediment supply is greatest, for example, along the path of the Madden Channel on the Hikurangi Margin (Figure 4). Along strike, that is, away from the primary depocentre, basin bounding structures, for example, the Pōrangahau Ridge, are more prominent, whilst internal deformation of basins is greater (Figures 5 and 14). Until the balance of sediment-structure interaction is lost, areas which receive high volumes of sediment may continue to focus stress on basin bounding structures, perpetuating growth of accommodation and leading to established depocentres. Eventually, even the basin bounding structures may become overwhelmed by sedimentation, supressing fault growth and forcing concentration of stress away from the loci of deposition. Concomitantly, this may lead to downstream bypass of sediment into newly forming depocentres, which in turn may supress deformation at this location and help propagate faulting further outboard. This migration of stress due to sediment loading may at least partly explain why the widest, least deformed part of the Hikurangi subduction wedge (McArthur et al., 2019) is the part traversed by the Madden depositional system, which has seen the most prolonged and largest volumes of sediment deposited in that part of the subduction wedge.

The type, volume and depositional architecture of sediment delivered to a basin also has significant effects on the style and distribution of deformation (Butler, 2019; Fillon et al., 2013; Marshak & Wilkerson, 1992; Noda, 2018; Storti & McClay, 1995; Teixell & Koyi, 2003). Basins that are relatively starved of sediment show more complex internal structure and closer fault spacing, for example, the Uruti Trough, along strike to the SW of the Pōrangahau Trough (McArthur et al., 2019). This complex structure in itself may inhibit sediment delivery to these areas, thus perpetuating local structure growth. However, the structural evolution of any area is further complicated by, amongst others factors, variation in structural style along strike (McArthur et al., 2019), subduction of seamounts (Collot et al., 2001) and the general rugosity of subducting strata, the presence and (over-) pressure of fluids

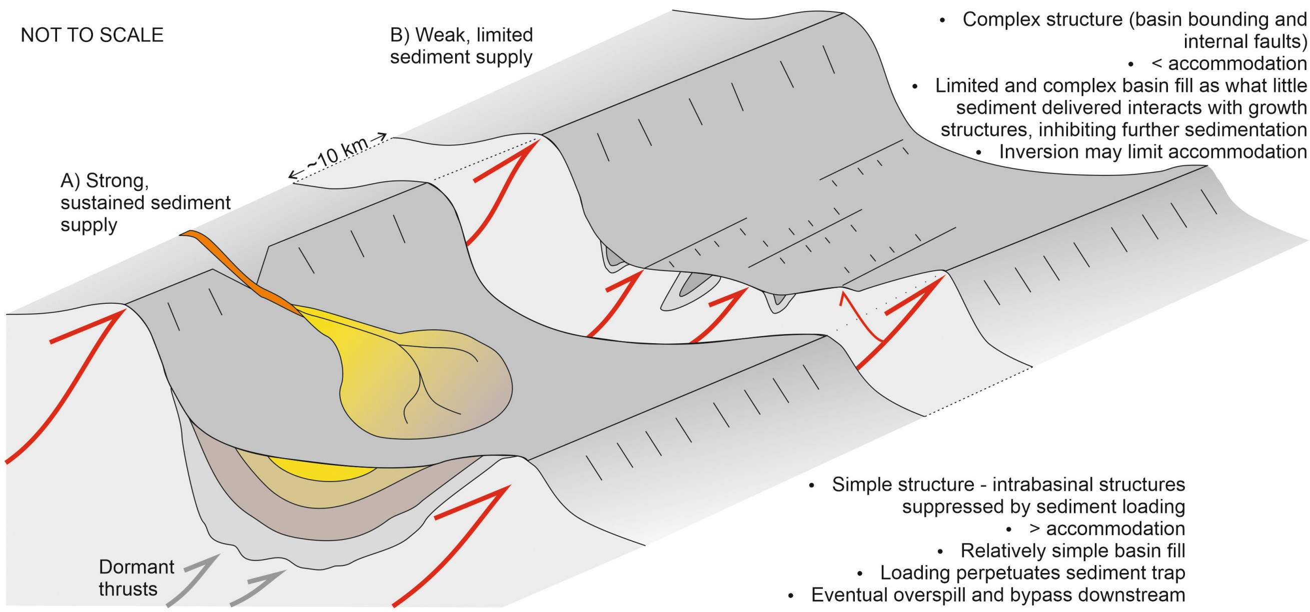

FIGURE 14 Schematic illustrations of the variable effect of (a) strong sediment supply and (b) weak sediment supply on the structural evolution of a fold and thrust belt basin.

(Hesse et al., 2010), variation in subduction velocity and obliquity (Nicol et al., 2007), and the nature of the plate interface (Barnes et al., 2020). Furthermore, erosion of sediment from a basin or overlying structures may cause reactivation of structures previously rendered inactive by sediment loading (e.g. Ballato et al., 2019; Steer et al., 2014), with out-of-sequence structure growth seen on this and other convergent margins (Bailleul et al., 2013; Chanier & Ferrière, 1991). The effects of sedimentation and erosion on strain localisation, fault distribution and evolution remain topics for further research, both on the Hikurangi and other active margins, where they may ultimately influence structural development of margins, accretionary prism development and plate boundary deformation.

6 | CONCLUSIONS

A 3D seismic study of 15,344 km^2 of data over the Hikurangi subduction margin demonstrates the complexity of intra-slope deep-water sedimentary system development over geological time. Five main sedimentary systems are described, across nine principal slope basins, plus numerous minor depocentres, spanning 75 km along strike and 75 km down dip, which were variably active through the Neogene until the present day.

Such sedimentary systems may vary temporally and spatially as their host tectonically active continental margin evolves. Both filling and spilling of intra-slope basins can occur simultaneously, as may the evolution of tortuous sediment dispersal corridors; however, these are considered end members. Hence a simple application of fill and spill' or 'tortuous corridor' models to tectonically active margins should be avoided.

At any one time a sedimentary system may be supplying a solitary basin, or multiple intra-slope basins, or completely bypassing the slope. Furthermore, 'filled' basins may begin accumulating sediment once more when creation of accommodation space is rejuvenated. Multiple and variably active sediment input points, with different sediment types along the margin result in the presence of variably complex and convolute depositional systems, often with similar styles of sedimentation occurring contemporaneously in proximal and distal basins, contrary to simple models of basin fill.

A hierarchy of external and internal controls on sediment distribution is recognised to dictate how sedimentation occurs in such slope basins: at the highest level sediment distribution is controlled by external factors, for example, glacio-eustacy, tectonic evolution of the margin, and the slope gradient. At an intermediate level, that is, individual basin scale, the interaction of sedimentary systems with evolving seafloor bathymetry, generated by structures and rugose MTD topography, can dictate the style of deposition, for example, whether a channel continues to propagate across the slope, or terminates in in a slope basin. At the lowest level, autocyclic factors (e.g. channel avulsion or flow stripping at sills) influence the spatiotemporal variation in erosion and sedimentation at any one place across the margin.

Finally, given that feedbacks have been recognised between faulting and adjacent sedimentation, constraining the distribution of sediment has major implications for understanding the tectonostratigraphic evolution of convergent margins. Areas of slope basins where sedimentation was focused have subdued structural deformation and become sites of enhanced sedimentation and more prospective hosts of natural resources. Conversely, structurally complex regions have limited and often disconnected sedimentary systems, which are less favourable for accumulations of natural resources or for geosolutions such as carbon capture and storage.

ACKNOWLEDGEMENTS

The sponsors of the Turbidites Research Group at the University of Leeds are thanked for funding this study, those being AkerBP, CNOOC, ConocoPhillips, Harbour, Murphy, OMV and Oxy. We thank WesternGeco for access to the data and permission to publish. Schlumberger and Ellis are respectively thanked for academic licences of Petrel and Paleoscan. Constructive reviews by Jess Hillman, Philip Barnes, Ian Kane, and an anonymous reviewer, along with the advice of Editor Atle Rotevatn, are gratefully acknowledged. Open access funding enabled and organized by ProjektDEAL.

PEER REVIEW

The peer review history for this article is available at https://publons.com/publon/10.1111/bre.12686.

DATA AVAILABILITY STATEMENT

The data that support the findings of this study are available from WesternGeco. Restrictions apply to the availability of these data, which were used under license for this study. Data are available from the authors with the permission of WesternGeco.

ORCID

Adam Daniel McArthur https://orcid.org/0000-0002-7245-9465

REFERENCES

Armitage, D. A., McHargue, T., Fildani, A., & Graham, S. A. (2012). Postavulsion channel evolution: Niger Delta continental slope Nigeria avulsions. *AAPG Bulletin*, *96*(5), 823–843.

Badalini, G., Kneller, B. C., & Winker, C. D. (2000). Architecture and processes in the late pleistocene Brazos-Trinity turbidite system, Gulf of Mexico continental slope. In *Deep-Water Reservoirs of the World: SEPM, Gulf Coast Section, 20th Annual Research Conference* (pp. 16–34).

Bailey, W. S., McArthur, A. D., & McCaffrey, W. D. (2020). Distribution of contourite drifts on convergent margins: Examples from the Hikurangi subduction margin of New Zealand. *Sedimentology*, *68*, 294–323.

Bailey, W. S., McArthur, A. D., & McCaffrey, W. D. (2021). Sealing potential of contourite drifts in deep-water fold and thrust belts: Examples from the Hikurangi Margin, New Zealand. *Marine and Petroleum Geology*, *123*, 104776.

Bailleul, J., Chanier, F., Ferrière, J., Robin, C., Nicol, A., Mahieux, G., Gorini, C., & Caron, V. (2013). Neogene evolution of lower trench-slope basins and wedge development in the central Hikurangi subduction margin, New Zealand. *Tectonophysics*, *591*, 152–174. https://doi.org/10.1016/j.tecto.2013.01.003

Bailleul, J., Robin, C., Chanier, F., Guillocheau, F., Field, B., & Ferrière, J. (2007). Turbidite systems in the inner forearc domain of the Hikurangi convergent margin (New Zealand): New constraints on the development of trench-slope basins. *Journal of Sedimentary Research*, *77*, 263–283. https://doi.org/10.2110/jsr.2007.028

Ballato, P., Brune, S., & Strecker, M. R. (2019). Sedimentary loading—Unloading cycles and faulting in intermontane basins: insights from numerical modeling and field observations in the NW Argentine Andes. *Earth and Planetary Science Letters*, *506*, 388–396.

Barnes, P. M., Ghisetti, F. C., Ellis, S., & Morgan, J. K. (2018). The role of protothrusts in frontal accretion and accommodation of plate convergence, Hikurangi subduction margin, New Zealand. *Geosphere*, *14*(2), 440–468. https://doi.org/10.1130/GES01552.1

Barnes, P. M., Lamarche, G., Bialas, J., Henrys, S., Pecher, I., Netzeband, G. L., Greinert, J., Mountjoy, J. J., Pedley, K., & Crutchley, G. (2010). Tectonic and geological framework for gas hydrates and cold seeps on the Hikurangi subduction margin, New Zealand. *Marine Geology*, *272*(1–4), 26–48. https://doi.org/10.1016/j.margeo.2009.03.012

Barnes, P. M., & Mercier de Lepinay, B. (1997). Rates and mechanics of rapid frontal accretion along the very obliquely convergent southern Hikurangi margin, New Zealand. *Journal of Geophysical Research*, *102*(B11), 24931–24952. https://doi.org/10.1029/97JB01384

Barnes, P. M., Nicol, A., & Harrison, T. (2002). Late cenozoic evolution and earthquake potential of an active listric thrust complex above the Hikurangi subduction zone, New Zealand. *Geological Society of America Bulletin*, *114*(11), 1379–1405.

Barnes, P. M., Wallace, L. M., Saffer, D. M., Bell, R. E., Underwood, M. B., Fagereng, A., & Meneghini, F. (2020). Slow slip source characterized by lithological and geometric heterogeneity. *Science Advances*, *6*(13), eaay3314.

Beanland, S., Melhuish, A., Nicol, A., & Ravens, J. (1998). Structure and deformational history of the inner forearc region, Hikurangi subduction margin, New Zealand. *New Zealand Journal of Geology and Geophysics*, *41*(4), 325–342. https://doi.org/10.1080/00288306.1998.9514814

Beaubouef, R. T., & Friedmann, S. J. (2000). High resolution seismic/sequence stratigraphic framework for the evolution of pleistocene intra slope basins, Western Gulf of Mexico: Depositional models and reservoir analogs. In *Deep-Water Reservoirs of the World: Gulf Coast Section SEPM 20th Annual Research Conference* (pp. 40–60).

Bland, K. J., Uruski, C. I., & Isaac, M. J. (2015). Pegasus Basin, eastern New Zealand: A stratigraphic record of subsidence and subduction, ancient and modern. *New Zealand Journal of Geology and Geophysics*, *58*, 319–343.

Booth, J. R., Dean, M. C., DuVernay, A. E., III, & Styzen, M. J. (2003). Paleo-bathymetric controls on the stratigraphic architecture and reservoir development of confined fans in the Auger Basin: central Gulf of Mexico slope. *Marine and Petroleum Geology*, *20*(6–8), 563–586.

Boulesteix, K., Poyatos-More, M., Flint, S. S., Taylor, K. G., Hodgson, D. M., & Hasiotis, S. T. (2019). Transport and deposition of mud in deep-water environments: Processes and stratigraphic implications. *Sedimentology*, *66*(7), 2894–2925.

Bourget, J., Zaragosi, S., Ellouz-Zimmermann, N., Mouchot, N., Garlan, T., Schneider, J. L., Lanfumey, V., & Lallemant, S. (2011). Turbidite system architecture and sedimentary processes along topographically complex slopes: The Makran convergent margin. *Sedimentology*, *58*(2), 376–406.

Bourget, J., Zaragosi, S., Ellouz-Zimmermann, S., Ducassou, E., Prins, M. A., Garlan, T., Lanfumey, V., Schneider, J. L., Rouillard, P., & Giraudeau, J. (2010). Highstand vs. lowstand turbidite system growth in the makran active margin: Imprints of high-frequency external controls on sediment delivery mechanisms to deep water systems. *Marine Geology*, *274*(1), 187–208.

Brooks, H. L., Hodgson, D. M., Brunt, R. L., Peakall, J., Poyatos-Moré, M., & Flint, S. S. (2018). Disconnected submarine lobes as a record of stepped slope evolution over multiple sea-level cycles. *Geosphere*, *14*(4), 1753–1779.

Brunt, R. L., McCaffrey, W. D., & Kneller, B. C. (2004). Experimental modeling of the spatial distribution of grain size developed in a fill-and-spill mini-basin setting. *Journal of Sedimentary Research*, *74*(3), 438–446.

Burgreen, B., & Graham, S. A. (2014). Evolution of a deep-water lobe system in the neogene trench-slope setting of the East Coast Basin, New Zealand: Lobe stratigraphy and architecture in a weakly confined basin configuration. *Marine and Petroleum Geology*, *54*, 1–22. https://doi.org/10.1016/j.marpetgeo.2014.02.011

Burgreen-Chan, B., Meisling, K. E., & Graham, S. A. (2016). Basin and petroleum system modelling of the East Coast Basin, New Zealand: A test of overpressure scenarios in a convergent margin. *Basin Research*, *28*(4), 536–567. https://doi.org/10.1111/bre.12121

Butler, R. W. H. (2019). Syn-Kinematic strata influence the structural evolution of emergent fold-thrust belts. *Geological Society, London, Special Publications*, *490*, SP490-2019.

Callec, Y., Deville, E., Desaubliaux, G., Griboulard, R., Huyghe, P., Mascle, A., Mascle, G., Noble, M., Padron de Carillo, C., & Schmitz, J. (2010). The Orinoco turbidite system: Tectonic controls on sea-floor morphology and sedimentation. *AAPG Bulletin*, *94*(6), 869–887.

Carter, L., Manighetti, B., Elliot, M., Trustrum, N., & Gomez, B. (2002). Source, sea level and circulation effects on the sediment flux to the deep ocean over the past 15 Ka off Eastern New Zealand. *Global and Planetary Change*, *33*(3–4), 339–355.

Chanier, F., & Ferrière, J. (1991). From a passive to an active margin; tectonic and sedimentary processes linked to the birth of an accretionary prism (Hikurangi Margin, New Zealand). *Bulletin de La Société Géologique de France*, *162*(4), 649–660.

Chanier, F., Ferrière, J., & Angelier, J. (1999). Extensional deformation across an active margin, relations with subsidence, uplift, and rotations: The Hikurangi subduction, New Zealand. *Tectonics*, *18*(5), 862–876. https://doi.org/10.1029/1999TC900028

Chen, H., Wood, L. J., & Gawthorpe, R. L. (2021). Sediment dispersal and redistributive processes in axial and transverse deep-time source-to-sink systems of Marine Rift Basins: Dampier sub-basin, Northwest Shelf, Australia. *Basin Research*, *33*(1), 227–249.

Clark, I. R., & Cartwright, J. A. (2009). Interactions between submarine channel systems and deformation in deepwater fold belts: Examples from the Levant Basin, Eastern Mediterranean Sea. *Marine and Petroleum Geology*, *26*(8), 1465–1482.

Claussmann, B., Bailleul, J., Chanier, F., Mahieux, G., Caron, V., McArthur, A. D., Chaptal, C., Morgans, H. E., & Vendeville, B. C. (2021). Shelf-derived mass-transport deposits: Origin and significance in the stratigraphic development of trench-slope basins. *New Zealand Journal of Geology and Geophysics*, *1-36*, 17–52. https://doi.org/10.1080/00288306.2021.1918729

Cohen, K. M., Finney, S. C., Gibbard, P. L., & Fan, J.-X. (2013). The ICS international chronostratigraphic chart. *Episodes*, *36*, 199–204.

Collot, J.-Y., Lewis, K., Lamarche, G., & Lallemand, S. (2001). The giant Ruatoria debris avalanche on the northern Hikurangi margin, New Zealand: Result of oblique seamount subduction. *Journal of Geophysical Research: Solid Earth*, *106*(B9), 19271–19297. https://doi.org/10.1029/2001JB900004

Crisóstomo-Figueroa, A., McArthur, A. D., Dorrell, R. M., Amy, L., & McCaffrey, W. D. (2021). A new modelling approach to sediment bypass prediction applied to the East Coast Basin, New Zealand. *GSA Bulletin*, *133*, 1734–1748.

Crutchley, G. J., Kroeger, K. F., Pecher, I. A., & Gorman, A. R. (2019). How tectonic folding influences gas hydrate formation: New Zealand's Hikurangi subduction margin. *Geology*, *47*(1), 39–42.

de Sagazan, C., & Olive, J.-A. (2021). Assessing the impact of sedimentation on fault spacing at the Andaman Sea Spreading Center. *Geology*, *49*(4), 447–451.

Deptuck, M. E., Sylvester, Z., O'byrne, C., & Prather, B. E. (2012). Pleistocene seascape evolution above a 'simple' stepped slope, western Niger Delta. *Application of the Principles of Seismic Geomorphology to Continental Slope and Base-of-Slope Systems: Case Studies from Sea Floor and near--Sea Floor Analog: SEPM Special Publication*, *99*, 199–222.

Doughty-Jones, G., Lonergan, L., Mayall, M., & Dee, S. (2019). The role of structural growth in controlling the facies and distribution of mass transport deposits in a deep-water salt minibasin. *Marine and Petroleum Geology*, *104*, 106–124.

Faugeres, J. C., Stow, D. A. V., Imbert, P., & Viana, A. (1999). Seismic features diagnostic of contourite drifts. *Marine Geology*, *162*(1), 1–38.

Fillon, C., Huismans, R. S., & van der Beek, P. (2013). Syntectonic sedimentation effects on the growth of fold-and-thrust belts. *Geology*, *41*(1), 83–86.

Ge, Z., Gawthorpe, R. L., Rotevatn, A., Zijerveld, L., Jackson, C. A. L., & Oluboyo, A. (2020). Minibasin depocentre migration during diachronous salt welding, Offshore Angola. *Basin Research*, *32*(5), 875–903.

Ge, Z., Gawthorpe, R. L., Zijerveld, L., & Oluboyo, A. P. (2021). Spatial and temporal variations in minibasin geometry and evolution in salt tectonic provinces: Lower Congo Basin, Offshore Angola. *Basin Research*, *33*(1), 594–611.

Ghisetti, F. C., Barnes, P. M., Ellis, S., Plaza-Faverola, A. A., & Barker, D. H. (2016). The last 2 Myr of accretionary wedge construction in the central Hikurangi margin (North Island, New Zealand): Insights from structural modeling. *Geochemistry, Geophysics, Geosystems*, *17*, 2661–2686.

Griffin, A. G., Bland, K. J., Morgans, H. E., & Strogen, D. P. (2021). A multifaceted study of the offshore Titihaoa-1 drillhole and a

Neogene accretionary slope basin, Hikurangi subduction margin. *New Zealand Journal of Geology and Geophysics*, *65*, 1–26. https://doi.org/10.1080/00288306.2021.1932527

Hansen, L., Hodgson, D. M., Pontén, A., Thrana, C., & Obradors Latre, A. (2021). Mixed axial and transverse deep-water systems: The Cretaceous Post-Rift Lysing formation, Offshore Norway. *Basin Research*, *33*, 2229–2251.

Hansen, L., Janocko, M., Kane, I., & Kneller, B. (2017). Submarine channel evolution, terrace development, and preservation of intra-channel thin-bedded turbidites: Mahin and Avon channels, offshore Nigeria. *Marine Geology*, *383*, 146–167.

Heron, D. W. (custodian). (2014). Geological map of New Zealand 1:250,000. Lower Hutt, NZ: GNS Science. *GNS Science Geological Map*, *1*, 1 CD.

Hesse, S., Back, S., & Franke, D. (2010). The structural evolution of folds in a deepwater fold and thrust belt—A case study from the Sabah Continental Margin Offshore NW Borneo, SE Asia. *Marine and Petroleum Geology*, *27*(2), 442–454.

Hillman, J. I., Cook, A. E., Daigle, H., Nole, M., Malinverno, A., Meazell, K., & Flemings, P. B. (2017). Gas hydrate reservoirs and gas migration mechanisms in the Terrebonne Basin, Gulf of Mexico. *Marine and Petroleum Geology*, *86*, 1357–1373.

Howlett, D. M., Gawthorpe, R. L., Ge, Z., Rotevatn, A., & Jackson, C. A. L. (2021). Turbidites, topography and tectonics: Evolution of submarine channel-lobe systems in the salt-influenced Kwanza Basin, offshore Angola. *Basin Research*, *33*, 1076–1110.

Howlett, D. M., Ge, Z., Nemec, W., Gawthorpe, R. L., Rotevatn, A., & Jackson, C. A. L. (2019). Response of unconfined turbidity current to deep-water fold and thrust belt topography: Orthogonal incidence on solitary and segmented folds. *Sedimentology*, *66*(6), 2425–2454.

Jiao, R., Seward, D., Little, T. A., & Kohn, B. P. (2014). Thermal history and exhumation of basement rocks from Mesozoic to Cenozoic subduction cycles, Central North Island, New Zealand. *Tectonics*, *33*(10), 1920–1935. https://doi.org/10.1002/2014TC003653

Kane, I. A., Clare, M. A., Miramontes, E., Wogelius, R., Rothwell, J. J., Garreau, P., & Pohl, F. (2020). Seafloor microplastic hotspots controlled by deep-sea circulation. *Science*, *368*(6495), 1140–1145.

Kneller, B. C., Dykstra, M., Fairweather, L., & Milana, J. P. (2016). Mass-transport and slope accommodation: Implications for turbidite sandstone reservoirs. *AAPG Bulletin*, *100*(2), 213–235.

Lee, J. M., & Begg, J. G. (2002). *Geology of the Wairarapa area: Institute of Geological & Nuclear Sciences 1:250,000 geological map 11. 1 sheet + 66 pages*. Institute of Geological and Nuclear Sciences Ltd.

Lewis, K. B., & Pettinga, J. R. (1993). The emerging, imbricate frontal wedge of the Hikurangi margin. *Sedimentary Basins of the World*, *2*, 225–250.

Marini, M., Patacci, M., Felletti, F., & McCaffrey, W. D. (2016). Fill to spill stratigraphic evolution of a confined turbidite mini-basin succession, and its likely well bore expression: The Castagnola Fm, NW Italy. *Marine and Petroleum Geology*, *69*, 94–111.

Marshak, S., & Wilkerson, M. S. (1992). Effect of overburden thickness on thrust belt geometry and development. *Tectonics*, *11*(3), 560–566.

Masek, J. G., & Duncan, C. C. (1998). Minimum-work mountain building. *Journal of Geophysical Research: Solid Earth*, *103*(B1), 907–917.

Mayall, M., Lonergan, L., Bowman, A., James, S., Mills, K., Primmer, T., Pope, D., Rogers, L., & Skeene, R. (2010). The response of turbidite slope channels to growth-induced seabed topography. *AAPG Bulletin*, *94*(7), 1011–1030.

McArthur, A. D., Bailleul, J., Chanier, F., Clare, A., & McCaffrey, W. D. (2021). Lateral, longitudinal, and temporal fill variation in trench-slope basins: Examples from the Neogene Akitio Sub-Bbasin, Hikurangi Margin, New Zealand. *New Zealand Journal of Geology and Geophysics*, *65*(1), 105–140. https://doi.org/10.1080/00288306.2021.1977343

McArthur, A. D., Bailleul, J., Mahieux, G., Claussmann, B., Wunderlich, A., & McCaffrey, W. D. (2021). Deformation-sedimentation feedback and the development of anomalously thick aggradational turbidite lobes: Outcrop and subsurface examples from the Hikurangi Margin, New Zealand. *Journal of Sedimentary Research*, *91*(4), 362–389. https://doi.org/10.2110/jsr.2020.013

McArthur, A. D., Claussmann, B., Bailleul, J., Clare, A., & McCaffrey, W. D. (2019). Variation in Syn-subduction sedimentation patterns from inner to outer portions of deep-water fold and thrust belts: Examples from the Hikurangi subduction margin of New Zealand. *Geological Society, London, Special Publications*, *490*, SP490-2018.

McArthur, A. D., & McCaffrey, W. D. (2019). Sedimentary architecture of detached deep-marine canyons: Examples from the East Coast Basin of New Zealand. *Sedimentology*, *66*, 1067–1101.

McArthur, A. D., & Tek, D. E. (2021). Controls on the origin and evolution of deep-ocean trench-axial channels. *Geology*, *49*(8), 883–888. https://doi.org/10.1130/G48612.1

McGilvery, T. A., & Cook, D. L. (2004). Flow paths and waterbottom gradients across a stepped slope profile, Offshore Brunei. *IPA-AAPG Deepwater and Frontier Symposium*, DFE04-PO-020, 463–469.

McKeown, M. (2018). *Understanding the physical sedimentology of the Madden continental slope distributary systems*. Unpublished MSc thesis. University of Auckland 135 pp.

Morley, C. K. (2009). Growth of folds in a deep-water setting. *Geosphere*, *5*(2), 59–89.

Mortimer, N. (2004). New Zealand's geological foundations. *Gondwana Research*, *7*(1), 261–272.

Naranjo-Vesga, J., Ortiz-Karpf, A., Wood, L., Jobe, Z., Paniagua-Arroyave, J. F., Shumaker, L., Mateus-Tarazona, D., & Galindo, P. (2020). Regional controls in the distribution and morphometry of deep-water gravitational deposits along a convergent tectonic margin. Southern Caribbean of Colombia. *Marine and Petroleum Geology*, *121*, 104639.

Nicol, A., & Beavan, J. (2003). Shortening of an overriding plate and its implications for slip on a subduction thrust, central Hikurangi margin, New Zealand. *Tectonics*, *22*(6), 1070.

Nicol, A., Mazengarb, C., Chanier, F., Rait, G., Uruski, C., & Wallace, L. (2007). Tectonic evolution of the active Hikurangi subduction margin, New Zealand, since the Oligocene. *Tectonics*, *26*(4), 1–24. https://doi.org/10.1029/2006TC002090

Noda, A. (2018). Forearc basin stratigraphy and interactions with accretionary wedge growth according to the critical taper concept. *Tectonics*, *37*(3), 965–988.

Olive, J. A., Behn, M. D., & Malatesta, L. C. (2014). Modes of extensional faulting controlled by surface processes. *Geophysical Research Letters*, *41*(19), 6725–6733.

Oluboyo, A. P., Gawthorpe, R. L., Bakke, K., & Hadler-Jacobsen, F. (2014). Salt tectonic controls on deep-water turbidite depositional systems: Miocene, Southwestern Lower Congo Basin, Offshore Angola. *Basin Research*, *26*(4), 597–620.

Paquet, F., Proust, J. N., Barnes, P. M., & Pettinga, J. R. (2011). Controls on active forearc basin stratigraphy and sediment fluxes: The Pleistocene of Hawke Bay, New Zealand. *GSA Bulletin*, *123*(5–6), 1074–1096.

Paumard, V., Bourget, J., Durot, B., Lacaze, S., Payenberg, T., George, A. D., & Lang, S. (2019). Full-volume 3D seismic interpretation methods: A new step towards high-resolution seismic stratigraphy. *Interpretation*, *7*(3), B33–B47.

Paumard, V., Bourget, J., Payenberg, T., George, A. D., Ainsworth, R. B., Lang, S., & Posamentier, H. W. (2020). Controls on deep-water sand delivery beyond the shelf edge: Accommodation, sediment supply, and deltaic process regime. *Journal of Sedimentary Research*, *90*(1), 104–130.

Pecher, I. A., Henrys, S. A., Wood, W. T., Kukowski, N., Crutchley, G. J., Fohrmann, M., Kilner, J., Senger, K., Gorman, A. R., Coffin, R. B., & Greinert, J. (2010). Focussed fluid flow on the Hikurangi Margin, New Zealand—Evidence from possible local upwarping of the base of gas hydrate stability. *Marine Geology*, *272*(1–4), 99–113.

Pettinga, J. R. (1982). Upper Cenozoic structural history, coastal southern Hawke's Bay, New Zealand. *New Zealand Journal of Geology and Geophysics*, *25*(2), 149–191.

Pirmez, C., Beaubouef, R. T., Friedmann, S. J., & Mohrig, D. C. (2000). Equilibrium profile and baselevel in submarine channels: Examples from late pleistocene systems and implications for the architecture of deepwater reservoirs. In *Deep-Water Reservoirs of the World: 20th Annual*, Deep-Water:782–805. Society of Economic Paleontologists and Mineralogists. https://doi.org/10.5724/gcs.00.15.0782.

Plaza-Faverola, A., Klaeschen, D., Barnes, P., Pecher, I., Henrys, S., & Mountjoy, J. (2012). Evolution of fluid expulsion and concentrated hydrate zones across the southern Hikurangi subduction margin, New Zealand: An analysis from depth migrated seismic data. *Geochemistry, Geophysics, Geosystems*, *13*(8), Q08018.

Plink-Björklund, P., & Steel, R. (2002). Sea-level fall below the shelf edge, without basin-floor fans. *Geology*, *30*(2), 115–118.

Posamentier, H. W., & Kolla, V. (2003). Seismic geomorphology and stratigraphy of depositional deep-water deposits 383. *Journal of Sedimentary Research*, *73*(3), 367–388. https://doi.org/10.1306/111302730367

Prather, B. E. (2003). Controls on reservoir distribution, architecture and stratigraphic trapping in slope settings. *Marine and Petroleum Geology*, *20*(6–8), 529–545.

Prather, B. E., Booth, J. R., Steffens, G. S., & Craig, P. A. (1998). Classification, lithologic calibration, and stratigraphic succession of seismic facies of intraslope basins, deep-water Gulf of Mexico. *AAPG Bulletin*, *82*(5a), 701–728.

Prather, B. E., O'Byrne, C., Pirmez, C., & Sylvester, Z. (2017). Sediment partitioning, continental slopes and base-of-slope systems. *Basin Research*, *29*(3), 394–416.

Prather, B. E., Pirmez, P., & Winker, C. D. (2012). Stratigraphy of linked intraslope basins: Brazos-Trinity system Western Gulf of Mexico. *Application of the Principles of Seismic Geomorphology to Continental-Slope and Base-of-Slope Systems: Case Studies from Seafloor and Near-Seafloor Analogues: SEPM, Special Publication*, *99*, 83–110.

Prelat, A., Hodgson, D. M., & Flint, S. S. (2009). Evolution, architecture and hierarchy of distributary deep-water deposits: A high-resolution outcrop investigation from the Permian Karoo Basin, South Africa. *Sedimentology*, *56*(7), 2132–2154. https://doi.org/10.1111/j.1365-3091.2009.01073.x

Rabouille, C., Dennielou, B., Baudin, F., Raimonet, M., Droz, L., Khripounoff, A., Martinez, P., Mejanelle, L., Michalopoulos, P., Pastor, L., & Pruski, A. (2019). Carbon and silica megasink in deep-sea sediments of The Congo Terminal Lobes. *Quaternary Science Reviews*, *222*, 105854.

Raine, J. I., Beu, A. G., Boyes, A. F., Campbell, H., Cooper, R. A., Crampton, J. S., Crundwell, M. P., Hollis, C. J., & Morgans, H. E. G. (2015). *Revised calibration of the New Zealand Geological Timescale*. NTGT2015/1: GNS Science, Lower Hutt, New Zealand.

Rait, G., Chanier, F., & Waters, D. W. (1991). Landward- and seaward-directed thrusting accompanying the onset of subduction beneath New Zealand. *Geology*, *19*(3), 230–233. https://doi.org/10.1130/0091-7613(1991)019<0230:LASDTA>2.3.CO;2

Reyners, M. (2013). The central role of the Hikurangi Plateau in the Cenozoic Tectonics of New Zealand and the Southwest Pacific. *Earth and Planetary Science Letters*, *361*, 460–468. https://doi.org/10.1016/j.epsl.2012.11.010

Satterfield, W. M., & Behrens, E. W. (1990). A late quaternary canyon/channel system, Northwest Gulf of Mexico Continental Slope. *Marine Geology*, *92*(1–2), 51–67.

Sheriff, R. E. (2002). *Encyclopedic dictionary of applied geophysics. Society of exploration geophysicists* (p. 442). SEG Books.

Sinclair, H. D., & Tomasso, M. (2002). Depositional evolution of confined turbidite basins. *Journal of Sedimentary Research*, *72*(4), 451–456.

Smith, R. (2004). Silled sub-basins to connected tortuous corridors; sediment distribution systems on topographically complex subaqueous slopes. In S. A. Lomas & P. Joseph (Eds.), *Confined Turbidite systems* (Vol. *222*, pp. 23–43). Geological Society of London Special Publication.

Soutter, E. L., Bell, D., Cumberpatch, Z. A., Ferguson, R. A., Spychala, Y. T., Kane, I. A., & Eggenhuisen, J. T. (2021). The influence of confining topography orientation on experimental turbidity currents and geological implications. *Frontiers in Earth Science*, *8*, 540633.

Spörli, K. B. (1980). New Zealand and oblique-slip margins: Tectonic development up to and during the Cainozoic. In P. F. Ballance & H. G. Reading (Eds.), *Sedimentation in oblique-slip mobile zones* (pp. 147–170). International Association of Sedimentologists, Special publications, no. 4.

Steer, P., Simoes, M., Cattin, R., & Shyu, J. B. H. (2014). Erosion influences the seismicity of active thrust faults. *Nature Communications*, *5*(1), 1–7.

Storti, F., & McClay, K. (1995). Influence of syntectonic sedimentation on thrust wedges in analogue models. *Geology*, *23*(11), 999–1002. https://doi.org/10.1130/0091-7613(1995)023%3C0999:IOSSOT%3E2.3.CO

Stow, D. A., Howell, D. G., & Nelson, C. H. (1985). Sedimentary, tectonic, and sea-level controls. In *Submarine fans and related turbidite systems* (pp. 15–22). Springer.

Strogen, D. P., Bland, K. J., Nicol, A., & King, P. R. (2014). Paleogeography of the Taranaki Basin Region during the Latest Eocene–Early Miocene and implications for the “Total Drowning” of Zealandia. *New Zealand Journal of Geology and Geophysics*, *57*(2), 110–127. https://doi.org/10.1080/00288306.2014.901231

Sylvester, Z., Cantelli, A., & Pirmez, C. (2015). Stratigraphic evolution of intraslope minibasins: Insights from surface-based model. *AAPG Bulletin*, *99*(6), 1099–1129.
Tap Oil Limited. (2004). *Tawatawa-1 Well Completion Report*. New Zealand Ministry of Economic Development Petroleum Series Report 3067. New Zealand, Wellington, p. 873.
Teixell, A., & Koyi, H. A. (2003). Experimental and field study of the effects of lithological contrasts on thrust-related deformation. *Tectonics*, *22*(5), 1054.
Tek, D. E., McArthur, A. D., Poyatos-Moré, M., Colombera, L., Allen, C., Patacci, M., & McCaffrey, W. D. (2021). Controls on the architectural evolution of deep-water channel overbank sediment wave fields: Insights from the Hikurangi Channel, offshore New Zealand. *New Zealand Journal of Geology and Geophysics*, *1-38*, 141–178. https://doi.org/10.1080/00288306.2021.1978509
Tek, D. E., Mcarthur, A. D., Poyatos-Moré, M., Colombera, L., Patacci, M., Craven, B., & Mccaffrey, W. D. (2021). Relating seafloor geomorphology to subsurface architecture: How mass-transport deposits and knickpoint-zones build the stratigraphy of the deep-water Hikurangi Channel. *Sedimentology*, *68*, 3141–3190. https://doi.org/10.1111/sed.12890
Tek, D. E., Poyatos-Moré, M., Patacci, M., McArthur, A. D., Colombera, L., Cullen, T. M., & McCaffrey, W. D. (2020). Syndepositional tectonics and mass-transport deposits control channelized, bathymetrically complex deep-water systems (Aínsa Depocenter, Spain). *Journal of Sedimentary Research*, *90*(7), 729–762. https://doi.org/10.2110/jsr.2020.38
Uruski, C. I. (1997). *Post-mortem on Titihaoa-1, Wairarapa*. Institute of Geological and Nuclear Sciences Science Report 97/31.
Vinnels, J. S., Butler, R. W., McCaffrey, W. D., & Paton, D. A. (2010). Depositional processes across the Sinú Accretionary Prism, Offshore Colombia. *Marine and Petroleum Geology*, *27*(4), 794–809.
Wallace, L. M., Beavan, J., McCaffrey, R., & Darby, D. (2004). Subduction zone coupling and tectonic block rotations in the North Island, New Zealand. *Journal of Geophysical Research: Solid Earth*, *109*(B12), B12406.
Wallace, L. M., Reyners, M., Cochran, U., Bannister, S., Barnes, P. M., Berryman, K., Downes, G., Eberhart-Phillips, D., Fagereng, A., Ellis, S., & Nicol, A. (2009). Characterizing the seismogenic zone of a major plate boundary subduction thrust: Hikurangi Margin, New Zealand. *Geochemistry, Geophysics, Geosystems*, *10*, Q10006.
Watson, S. J., Mountjoy, J. J., & Crutchley, G. J. (2020). Tectonic and geomorphic controls on the distribution of submarine landslides across active and passive margins, Eastern New Zealand. *Geological Society, London, Special Publications*, *500*(1), 477–494.
Willett, S. D. (1999). Orogeny and orography: The effects of erosion on the structure of mountain belts. *Journal of Geophysical Research: Solid Earth*, *104*(B12), 28957–28981.
Worthington, L. L., Daigle, H., Clary, W. A., Gulick, S. P., & Montelli, A. (2018). High sedimentation rates and thrust fault modulation: Insights from Ocean Drilling Offshore the St. Elias Mountains, Southern Alaska. *Earth and Planetary Science Letters*, *483*, 1–12.
Wynn, R. B., & Stow, D. A. V. (2002). Classification and characterisation of deep-water sediment waves. *Marine Geology*, *192*(1–3), 7–22.

SUPPORTING INFORMATION

Additional supporting information can be found online in the Supporting Information section at the end of this article.

How to cite this article: McArthur, A. D., Crisóstomo-Figueroa, A., Wunderlich, A., Karvelas, A., & McCaffrey, W. D. (2022). Sedimentation on structurally complex slopes: Neogene to recent deep-water sedimentation patterns across the central Hikurangi subduction margin, New Zealand. *Basin Research*, *34*, 1807–1837. https://doi.org/10.1111/bre.12686